RcsF-independent mechanisms of signaling within the Rcs Phosphorelay

Short title: RcsF-independent signaling by the Rcs Phosphorelay

Anushya Petchiappan[1], Nadim Majdalani[1], Erin Wall[1, 2] and Susan Gottesman[1, *]

[1]Laboratory of Molecular Biology, Center for Cancer Research, National Cancer Institute, Bethesda, MD., 20892

[2]Current address: US Food and Drug Administration, Office of Pharmaceutical Quality, Silver Spring MD 20903

***Corresponding author: Susan Gottesman: gottesms@mail.nih.gov**

Keywords: Cell surface stress, RcsF, DsbA, DjlA, two-component signaling

Abstract:

The Rcs (regulator of capsule synthesis) phosphorelay is a conserved cell envelope stress response mechanism in enterobacteria. It responds to perturbations at the cell surface and the peptidoglycan layer from a variety of sources, including antimicrobial peptides, beta-lactams, and changes in osmolarity. RcsF, an outer membrane lipoprotein, is the sensor for this pathway and activates the phosphorelay by interacting with an inner membrane protein IgaA. IgaA is essential; it negatively regulates the signaling by interacting with the phosphotransferase RcsD. We previously showed that RcsF-dependent signaling does not require the periplasmic domain of the histidine kinase RcsC and identified a dominant negative mutant of RcsD that can block signaling via increased interactions with IgaA. However, how the inducting signals are sensed and how signal is transduced to activate the transcription of the Rcs regulon remains unclear. In this study, we investigated how the Rcs cascade functions without its only known sensor, RcsF and characterized the underlying regulatory mechanisms for three distinct RcsF-independent inducers. Previous reports showed that Rcs signaling can be induced in the absence of RcsF by a loss of function mutation in the periplasmic oxidoreductase DsbA or by overexpression of the DnaK cochaperone DjlA. We identified an inner membrane protein, DrpB, as a multicopy RcsF-independent Rcs activator in *E. coli*. The loss of the periplasmic oxidoreductase DsbA and the overexpression of the DnaK cochaperone DjlA each trigger the Rcs cascade in the absence of RcsF by weakening IgaA-RcsD interactions in different ways. In contrast, the cell-division associated protein DrpB uniquely requires the RcsC periplasmic domain for signaling; this domain is not needed for RcsF-dependent signaling. This suggests the possibility that RcsC acts as a sensor for some Rcs signals. Overall, the results add new understanding to how this complex phosphorelay can be activated by diverse mechanisms.

Author summary:

The Rcs phosphorelay signaling cascade regulates the expression of genes related to capsule synthesis, biofilm formation, virulence, and cell division in Enterobacteria and is critical for cell membrane integrity and response to beta-lactam antibiotics and antimicrobial peptides. RcsF is the sole known sensor, but other

43 proteins have been reported to activate this pathway in the absence of RcsF. We have discovered a novel
44 RcsF-independent Rcs activator and found that each of three RcsF-independent proteins activate the system
45 differently. Most significantly, we find that the histidine kinase RcsC can be involved in signal sensing
46 independently of RcsF. Our study sheds light into the complex mechanisms of Rcs activation and adds to
47 our knowledge of non-orthodox signaling systems across organisms.
48
49
50 **Introduction**
51 The Gram-negative bacterial cell wall envelope comprises an outer membrane, the periplasm, a
52 peptidoglycan layer, and an inner membrane [1]. It serves as a protective barrier against environmental
53 insults and a permeability barrier for selective uptake of nutrients. Due to its structural and functional
54 importance for growth and metabolism, bacteria have evolved a multitude of envelope stress response
55 systems to monitor various stresses at the cell wall and respond to them in a timely manner. These systems
56 typically contain a sensor protein which detects the stressor and subsequently activates the downstream
57 signaling pathway leading to changes in gene transcription. A highly conserved envelope stress response
58 pathway in enterobacteria is the Rcs phosphorelay [2]. This cascade responds to outer membrane and
59 peptidoglycan stress from both external and intrinsic sources. While Rcs is a member of the ubiquitous
60 histidine kinase/response regulator signaling systems, in which phosphorylation of the response regulator
61 regulates output, it is significantly more complex than the canonical two-component signaling systems,
62 making it a unique but challenging model to study non-orthodox signaling systems across organisms.
63 The Rcs pathway has been shown to be activated in response to beta-lactams, antimicrobial
64 peptides, osmotic shock, acid stress, defects in LPS trafficking, peptidoglycan biosynthesis, and contact
65 with a solid surface. The Rcs regulon was first defined for its role in regulating synthesis of capsular
66 polysaccharide but has been shown to include genes related to biofilm formation, motility, virulence, cell
67 morphology, and cell division, among others (reviewed in [2]). How Rcs responds to a wide array of

68 inducers, and the exact mechanism of signal sensing and transduction remains unclear; structural
69 information about most of the components is currently lacking.

70 The multi-step Rcs phosphorelay comprises an inner membrane hybrid histidine kinase RcsC, an
71 inner membrane phosphotransfer protein RcsD, and the response regulator RcsB (Fig. 1A). The sensor for
72 this cascade is an outer membrane lipoprotein RcsF [3-5]. RcsF detects LPS/peptidoglycan defects and
73 chemical stressors like polymyxin B (presumed to disrupt LPS), A22 (a MreB inhibitor), and mecillinam
74 (a beta-lactam antibiotic) [6, 7]. The phosphorelay is negatively regulated by inner membrane protein IgaA.
75 IgaA is essential and it can only be deleted if the phosphorelay is inactivated by mutations in *rscC*, *rcsD*,
76 or *rcsB* [8]. During normal growth, IgaA represses signaling by interacting with RcsD. When RcsF
77 perceives stress at the envelope, it activates signaling by interacting with the periplasmic domain of IgaA.
78 This relieves the repression of signaling by IgaA, presumably changing the way in which RcsD interacts
79 with RcsC to induce the phosphorelay. A required step in the phosphorelay activation is the
80 autophosphorylation of RcsC. RcsC is a complex histidine kinase, with a receiver domain with a conserved
81 aspartate at its C-terminus (Fig. 1A). A phosphate group is transferred from the conserved histidine residue
82 in RcsC to the aspartate within the RcsC receiver domain. This phosphate group is then transferred to a
83 conserved histidine residue in RcsD and subsequently to an aspartate in RcsB. Phosphorylated RcsB dimers
84 bind promoters to regulate transcription. Alternatively, RcsB can act in concert with other auxiliary partners
85 like RcsA to regulate gene expression (reviewed in [2]). IgaA and RcsD contact each other both in the
86 periplasm and in the cytoplasm; weakening of either interaction leads to activation of the phosphorelay [9].
87 Thus, IgaA provides a braking mechanism, with the cytoplasmic contact with RcsD as the regulatory switch
88 and the periplasmic interaction preventing Rcs over-activation. The identification of the cytoplasmic
89 interaction as the likely regulatory switch was further underscored by our isolation of a dominant mutation
90 in *rcsD* in its cytoplasmic PAS-like domain (T411A) [9]. The RcsD T411A mutation blocks induction by
91 polymyxin B nonapeptide (PMBN) and other inducers due to tightened cytoplasmic interaction with IgaA.

92 While the histidine kinase is the sensor for most two-component systems, RcsC is not known to be
93 a sensor for any of the known Rcs signals. Consistent with this, we previously demonstrated that the RcsC

94 periplasmic domain is dispensable for polymyxin B nonapeptide (PMBN) induction of the Rcs cascade [9].
95 The outer membrane lipoprotein RcsF remains the only known sensor of the system. RcsF resides within
96 the lumen of the OMP such that a portion of it is surface-exposed [5, 10, 11]. RcsF activates Rcs upon
97 sensing signals perturbing the cell surface and the peptidoglycan layer or upon its mislocalization to the
98 inner membrane.

99 While the majority of inducing signals require RcsF, there are a number of situations in which
100 RcsF-independent activation of Rcs has been reported. Overexpression of the DnaK cochaperone protein
101 DjlA activates Rcs even in the absence of RcsF [12, 13]. Loss-of-function mutations in *dsbA*, encoding a
102 periplasmic oxidoreductase, also activate the phosphorelay independently of RcsF [4]. Overproduction or
103 mutation of a number of proteins, including TolB [14], DrpB [15], YpdI [16], YmgABC [17], YfgM [18,
104 19] and YqjA [20], have been linked with Rcs activation but the role of RcsF for signaling has not been
105 reported [4]. Given the complexity of the Rcs phosphorelay, it seems possible that RcsF-independent
106 activation reflects the existence of additional signaling pathways.

107 Here, we further investigated the nature of RcsF-independent signaling in *dsbA* mutants and upon
108 *djlA* overproduction. We performed a screen for novel RcsF-independent Rcs activators and uncovered a
109 third pathway for RcsF-independent signaling. Comparisons between these pathways delineated three
110 genetically distinct modes of Rcs induction, demonstrating that they are also mechanistically distinct,
111 revealing novel aspects of the regulation of the phosphorelay and implicating the RcsC periplasmic domain
112 in one of these signaling pathways.

113

114 **Results**

115 **DrpB is a novel RcsF-independent Rcs activator**

116 With the aim of identifying novel proteins capable of triggering the Rcs cascade in an RcsF-independent
117 manner, we utilized a fluorescence-based genetic screen in *E. coli*. We transformed a plasmid library
118 carrying 3-5 kb fragments of the *E. coli* chromosome into strain EAW34, carrying a reporter for Rcs
119 activation and deleted for *rcsF*. The reporter used is a transcriptional fusion of the *rprA* promoter, an RcsB

120 target, to the mCherry protein, referred to here as P_{rprA}::mCherry [9, 21]. This strain normally shows low
121 fluorescence in the absence of RcsF, due to low Rcs signaling. The colonies were screened for increased
122 fluorescence and 14 plasmids containing putative RcsF-independent Rcs activators were isolated.
123 Sequencing of the plasmids revealed that 13 of them contained overlapping fragments of the *E. coli*
124 chromosome that included genes encoding the YedR (DrpB) ORF along with the RseX sRNA (Fig. S1A).
125 The remaining plasmid contained genes encoding the YihA protein and the sRNAs Spot 42 and CsrC (Fig.
126 S1B). We previously reported that overexpression of Spot42 induces the Rcs pathway and while that study
127 suggested that much of the Spot 42 effect was RcsF dependent, only a qualitative assay was done [21]. Spot
128 42, an Hfq-dependent regulatory RNA, regulates translation and stability of multiple mRNAs and has
129 pleiotropic effects in the cell making identification of a single critical target complicated.

130 To further validate identification of DrpB as capable of RcsF-independent induction, we assayed
131 the growth and fluorescence of wildtype, Δ*rcsF* and Δ*rcsB* strains expressing DrpB or the known RcsF-
132 independent activator DjlA under control of the arabinose-inducible pBAD promoter, using the same
133 P_{rprA}::mCherry fusion as a reporter for Rcs activation. Overexpression of both DrpB and DjlA showed
134 increased fluorescence, both in the presence and absence of RcsF, confirming their role as multicopy RcsF-
135 independent Rcs activators (Fig. 1B). The increased fluorescence was fully dependent on RcsB for both
136 genes. We did not observe a significant RcsF-independent induction by YihA or *rseX*, and the modest
137 induction by Spot42 in Δ*rcsF* was also not significant (Fig. S1C and S1D). Therefore, we focused our
138 investigation on DrpB. DrpB is a small inner membrane protein and was previously found to activate both
139 the Rcs and the Psp stress response upon overexpression, suggesting that its overexpression leads to
140 membrane stress [15].

141 We also confirmed that the deletion of *dsbA* activates the Rcs pathway in an RcsF-independent
142 manner, by measuring the fluorescence of the same P_{rprA}::mCherry reporter in Δ*dsbA,* Δ*dsbA* Δ*rcsF*, and
143 Δ*dsbA* Δ*rcsB* strains (Fig. 1C). Deletion of *dsbA* increased the basal P_{rprA}::mCherry activity independently
144 of RcsF but not RcsB. Strains devoid of DsbA are defective in disulfide bond formation in periplasmic

145 proteins and DTT treatment is known to exacerbate this problem. Addition of DTT further induced the Rcs
146 pathway, but only in the absence of DsbA. Unexpectedly, we found that PMBN, which normally induces
147 the pathway in an RcsF-dependent-fashion (see WT and Δ*rcsF* results in Fig. 1C), also induced this
148 pathway, to a similar extent as DTT, in both Δ*dsbA* and Δ*dsbA* Δ*rcsF* strains (Fig. 1C). Together, these
149 results provide evidence for three RcsF-independent Rcs signaling situations – lack of DsbA and
150 overproduction of DjlA or DrpB.

151 We next investigated whether these inducers of Rcs signaling depend on each other. We first
152 measured the Rcs signaling in *dsbA* mutants in cells also deleted for the chromosomal copies of *djlA* or
153 *drpB* (Fig. S2A). Signaling in the Δ*dsbA* Δ*djlA* and Δ*dsbA* Δ*drpB* strains was essentially unchanged from
154 that seen in the Δ*dsbA* strain (see Fig. 1C). Therefore, the absence of DsbA does not signal by mimicking
155 overexpression of DjlA or DrpB. In addition, overexpression of DjlA or DrpB induces signaling in a *dsbA*
156 deletion strain (Fig. S2B), although the overexpression of DrpB led to poor growth in the absence of DsbA
157 (see OD values, Fig S2B). We also tested if the multicopy activators DjlA and DrpB require each other to
158 trigger Rcs signaling and found that they did not (Fig. S2C). Together, these results indicate that DsbA,
159 DjlA, and DrpB do not require one another for signaling and possibly employ different mechanisms of Rcs
160 activation. We next investigated the pathways they each use for RcsF-independent activation of Rcs.

161

162 **DrpB has a unique requirement for the RcsC periplasmic domain for signaling**

163 The Rcs pathway can be activated simply by increasing the levels of RcsB [22]. If this were how the RcsF-
164 independent factors were working, they might be independent of the histidine kinase, RcsC and the
165 phosphotransfer protein RcsD. Previous work had demonstrated that multicopy DjlA and DrpB are still
166 dependent on RcsC for signaling [12, 13, 15]. As seen in Fig. 2, while deletion of *rcsC* caused an increase
167 in the basal level of P_{rprA}::mCherry expression, as previously seen [9, 21], there was no further induction in
168 the absence of RcsC for any of these factors.

169 We previously showed that the RcsC periplasmic domain is not needed for the RcsF-dependent
170 PMBN response [9]. We assayed the Rcs activation upon deletion of *dsbA* or overexpression of DjlA or
171 DrpB in strains encoding a chromosomal version of RcsC missing its periplasmic domain (*rcsC* Δ*peri*).
172 Fig. 2A shows that PMBN was able to induce signaling in the *rcsC* Δ*peri* strain as previously found.
173 Deletion of *dsbA* in the *rcsC* Δ*peri* strain increased the basal level of signaling, although not to the extent
174 seen for the *rcsC*$^+$ strain (Δ*dsbA*); DTT or PMBN further increased signaling (Fig. 2A). These results
175 demonstrate that the effect of Δ*dsbA* is independent of the RcsC periplasmic region. DjlA overexpression
176 was also able to activate signaling in the *rcsC* Δ*peri* strain (Fig. 2B). However, upon DrpB overexpression,
177 no Rcs activation was observed in the *rcsC* Δ*peri* strain (Fig. 2B). This is the first evidence of a role for the
178 RcsC periplasmic domain in signaling and provides clear evidence that DrpB acts in a manner that is distinct
179 from DjlA overexpression or loss of DsbA.
180
181 **DjlA, but not DsbA and DrpB, can induce Rcs signaling in a RcsD T411A mutant**
182 As for deletion of *rcsC* (Fig. 2), all three factors were unable to induce signaling in the absence of the
183 phosphorelay protein RcsD (Fig. 3). RcsD T411A is an allele of RcsD expressing a mutant in the
184 cytoplasmic domain of RcsD that has a higher affinity for IgaA, blocking RcsF-dependent PMBN signaling
185 [9] (Fig. 3A). Strains carrying *rcsD* T411A were used to further explore the role of IgaA-RcsD interactions
186 in RcsF-independent signaling. DsbA signaling was blocked by the *rcsD* T411A mutation; the basal level
187 was reduced to that seen in *rcsD* T411A alone, and the DTT or PMBN increase was blocked (Fig. 3A).
188 Overexpression of DrpB also could not induce signaling in the *rcsD* T411A strain (Fig. 3B). However,
189 DjlA overexpression activated signaling in this strain, indicating its unique ability to overcome the effect
190 of the *rcsD* T411A mutation.
191 We considered the possibility that DjlA could function in the *rcsD* T411A strain because it was the
192 strongest inducer of the conditions tested. As seen in Fig. 1B and 1C, DjlA overexpression gave around 30-
193 fold induction, which is higher than DrpB overexpression (~17 fold), DsbA deletion (~13 fold), and the

194 RcsF-dependent response to PMBN (~4 fold). As a test of this model, we examined the ability of RcsD
195 T411A to block signaling when RcsF is highly active. Overproduction of RcsF or expression of a derivative
196 ($RcsF^{IM}$, carrying mutations S17D and M18Q) that localizes the protein to the inner member and
197 constitutively activates Rcs signaling [7, 23] both induce Rcs signaling, with the inner-membrane localized
198 mutant RcsF derivative, $RcsF^{IM}$, being the stronger activator, inducing better than 25-fold (Fig.S3).
199 However, the T411A mutation was still able to block this signaling (Fig. S3). These results suggest that
200 DjlA is unique in its ability to fully overcome the *rcsD* T411A allele.
201 Thus, each of the three RcsF-independent factors has distinct patterns of induction, suggesting that
202 they act in different manners. While all three are dependent upon RcsC and RcsD, only DrpB signaling
203 depends on the RcsC periplasmic domain and only DjlA can bypass the *rcsD* T411A allele to induce
204 signaling. Below we further examine how each of these factors works.
205
206 **DsbA is needed for efficient IgaA-RcsD periplasmic interactions**
207 DsbA resides in the periplasm and plays a central role in disulfide bond (DSB) formation in *E. coli* and
208 other bacteria [reviewed in [24]]. DsbA, in concert with DsbB, introduces disulfide bonds into newly
209 synthesized periplasmic proteins, predominantly between consecutive cysteine residues [25-27]. *dsbA* null
210 mutants show a pleotropic phenotype consistent with defects in the cell envelope - they are mucoid, non-
211 motile, sensitive to DTT as well as some drugs, show decreased fitness and attenuated virulence [24, 25,
212 28, 29]. Periplasmic and membrane proteins that require disulfide bonds frequently require DsbA for proper
213 folding. One such protein is the Rcs sensor protein, the outer membrane lipoprotein RcsF [30]. RcsF has
214 two non-consecutive disulfide bridges and impaired disulfide bond formation leads to its degradation [31,
215 32]. Thus, RcsF is non-functional in a *dsbA* mutant, supporting the idea that mucoidy in the *dsbA* mutant
216 strain, likely reflecting Rcs induction, cannot be due to activation via RcsF; this is confirmed by the
217 induction of the P_{rprA}::mCherry reporter in the absence of RcsF in Fig. 1C. This is further validated by the
218 absence of Rcs induction in response to Mecillinam or the MreB inhibitor A22 by the *dsbA* mutants, both
219 dependent on RcsF (Fig. S4A). Note that this result also distinguishes PMBN from these other inducers as

220 uniquely still able to induce the Rcs phosphorelay in the *dsbA* mutant (Fig. 2A, Fig. S4B; compare
221 differences in fold induction).

222 Aside from RcsF, RcsC, RcsD, and IgaA each have a periplasmic domain that could possibly be
223 targets for DsbA. RcsD does not have any conserved cysteine residues within its periplasmic domain, ruling
224 it out as a direct target of DsbA.

225 RcsC has two conserved cysteine residues in its periplasmic domain, but since the *ΔdsbA rcsC*
226 Δ*peri* strain is still DTT-inducible (Fig. 2A), this cannot be the critical target for DsbA. However, our results
227 do suggest that, directly or indirectly, the RcsC periplasmic domain contributes to phosphorelay activation
228 in the absence of DsbA. While deletion of the RcsC periplasmic domain had only a modest effect on
229 P_{rprA}::mCherry basal level or induction in a *dsbA*$^+$ strain (compare WT to *rcsC*Δ*peri* data, Fig. 2A), levels
230 of expression in the Δ*dsbA* mutants were significantly lower for Δ*dsbA rcsC* Δ*peri* than for Δ*dsbA rcsC*$^+$
231 (Fig. 2A), with Δ*dsbA* 12-fold higher than WT in the absence of induction, while Δ*dsbA rcsC*Δ*peri* was
232 only 3.2-fold increased compared to WT or *rcsC*Δ*peri* (Fig. 2A). To determine if this reduction in induction
233 was dependent upon RcsC disulfide bonds, we examined the behavior of a strain expressing RcsC mutant
234 for the C111 and C154 periplasmic cysteine residues (*rcsC C111A C154A*, named here as *rcsC C2A*) in
235 *dsbA*$^+$ or *ΔdsbA* strains. As seen in Fig. S4B, the *rcsC C2A dsbA*$^+$ strain has the same pattern of expression
236 as the WT strain or a *rcsC* Δ*peri* strain (Fig.2A), responding to PMBN but not DTT. The *ΔdsbA rcsC C2A*
237 strain, unlike the *rcsC*Δ*peri* strain, responds to both DTT and PMBN and this response is not muted as in
238 *rcsC*Δ*peri* (compare to Fig. 2A). This suggests the effect of the *rcsC* Δ*peri* does not reflect a role of the
239 RcsC periplasmic cysteine residues and is likely more indirect; this was not further explored here.

240 IgaA has four conserved periplasmic cysteine residues, suggesting that there are two disulfide
241 linkages in its periplasmic domain. A study in *Salmonella* supported the idea that at least the first of the
242 disulfide bonds was important for proper IgaA function [33]. Given that IgaA is essential, the *dsbA* mutant
243 cannot lead to fully non-functional IgaA. However, if the disulfide bonds are not properly formed, the
244 periplasmic interaction between IgaA and RcsD could be affected in the absence of DsbA, leading to the

245 observed Rcs activation. We have previously shown that IgaA and RcsD interact in a bacterial two hybrid
246 (BACTH) assay, and that the interaction detected by this assay is primarily dependent upon a periplasmic
247 contact between the proteins [9]. This assay is based on the reconstitution of the Bordetella adenylate
248 cyclase from its two fragments, T18 and T25, in an adenylate cyclase mutant (*cya*) strain BTH101 [34, 35].
249 Fusion of each of these fragments to an interacting protein reconstitutes adenylate cyclase, assayed by the
250 Cya-dependent synthesis of beta-galactosidase. Both orientations, IgaA-T18/RcsD-T25 as well as IgaA-
251 T25/RcsD-T18, have been demonstrated to show a strong interaction ([9] and Fig. 4A, WT strain).

252 We introduced the *dsbA* null mutant into the host for the BACTH assay and studied its effect on
253 the IgaA-RcsD interaction, compared to the WT strain (Fig. 4A). The interaction between IgaA and RcsD
254 was significantly impaired in the *dsbA* mutant, suggesting that DsbA is needed to maintain a proper IgaA-
255 RcsD interaction, possibly due to its role in IgaA folding. Given the localization of DsbA in the periplasm,
256 we would expect that it is the periplasmic interaction of IgaA with RcsD that should be defective in the
257 absence of DsbA. This was confirmed first by testing the interaction of RcsD with various domain deletion
258 constructs of IgaA. IgaA has five transmembrane helices anchoring two cytoplasmic domains and a large
259 periplasmic domain (schematic in Fig. 4B). The IgaA Δ*peri* (Δ384-649) protein has been shown to have a
260 weak interaction with RcsD, confirmed here; loss of DsbA did not further decrease the interaction (Fig.
261 4B). Deletion of the two cytoplasmic domains (IgaA Δcyt), on the other hand, did not decrease the
262 interaction, but was very sensitive to loss of DsbA (Fig. 4B). Neither of these deletions significantly affected
263 the levels of expression of the IgaA-T18 protein, in the presence of absence of DsbA (Fig. S4D). This data
264 is best explained by a change in the IgaA periplasmic domain in the absence of DsbA, reducing the
265 periplasmic interaction with RcsD.

266 A crystal structure of the *E. coli* IgaA periplasmic domain shows the presence of the two disulfide
267 linkages to be C404-C425 and C498-C504, consistent with previous work [33, 36]. We mutated the
268 Cysteine residues to Serine and tested their effect on the IgaA-RcsD interaction, either in pairs (C404S
269 C425S or C498S C504S) or in a mutant with all four mutated (C4S) (Fig. S4C). Breaking either linkage

270 significantly weakened the interaction of IgaA with RcsD. As with the data for Δ*dsbA* in Fig. 4B, the RcsD
271 T411A allele overcame much (but not all) of the loss of interaction in the IgaAC4S derivative (Fig. S4C).
272 Therefore, for this interaction assay, C4S mimics the effect of loss of *dsbA*, supporting the idea that the
273 disulfide linkages are required for proper folding of the periplasmic domain of IgaA and its periplasmic
274 interaction with RcsD. Mutations in IgaA may lead to its degradation during the stationary phase [33] but
275 the overexpressed IgaA C4S mutant was stable in the T18 fusion, suggesting DsbA primarily affects its
276 folding (Fig. S4D).

277 The prediction from these interaction assays is that mutations of the IgaA cys residues should also
278 lead to increased activation of the Rcs phosphorelay, as seen for Δ*dsbA* in the presence of DTT. The
279 chromosomal copy of *igaA* was replaced with *igaA*C4S in an *rcsD* mutant strain carrying the P_{rprA}::mCherry
280 reporter. While this strain (AP168) is not fluorescent and is non-mucoid, due to lack of RcsD, when a
281 plasmid carrying RcsD was introduced into the cells, colonies became mucoid, consistent with activation
282 of the Rcs phosphorelay. Growth was poor and it seems likely that this C4S strain, like other strains that
283 express the Rcs phosphorelay at high levels, rapidly picks up suppressing mutations. Growing the
284 transformed colonies without further purification in LB and assaying the P_{rprA}::mCherry signal
285 demonstrated that the signal was higher than that seen with the Δ*dsbA* strain and was not affected by DTT
286 (Fig. S4E). Thus, blocking disulfide bond formation in IgaA via mutation of the cysteine residues induces
287 Rcs signaling and mimics the Δ*dsbA* phenotype. Because either pair of cysteine mutants abrogates the full
288 interaction with RcsD (Fig. S4C), it seems likely both disulfide bonds are important for proper IgaA folding.
289

290 **DjlA can act as a cochaperone and mediate IgaA-RcsD cytoplasmic interactions**

291 DjlA is the third member of the DnaJ domain family in *E. coli*. Proteins with this domain, including DnaJ
292 and CbpA in *E. coli*, collaborate as part of the widely conserved DnaK/Hsp70 chaperone network. DjlA is
293 localized at the cytoplasmic membrane with a short N-terminal region in the periplasm followed by a single
294 transmembrane helix [37]. The conserved J-domain, needed for DnaK interaction, is in the cytoplasm at the

295 C-terminal. A TerB-like (tellurite resistance) domain of unknown function lies between the J-domain and
296 the membrane helix. The role played by this domain has not been clearly defined but it has been speculated
297 to be involved in membrane/lipid-interaction, stress-sensing, DNA processing, and phage defense [38, 39].
298 Although the precise cellular function and substrates of DjlA are unknown, it is a bonafide DnaK
299 cochaperone capable of assisting DnaK in protein refolding [40]. DjlA is not essential for growth and a null
300 mutant did not reveal any significant phenotype except a delayed onset of mucoidy at low temperature [13].
301 On the other hand, overproduction of DjlA was clearly toxic, with the cells exhibiting growth defects
302 suggestive of a role of DjlA in cell division or membrane integrity [37]. Furthermore, strains overexpressing
303 DjlA demonstrated increased capsule synthesis, as result of Rcs activation, and hypersensitivity to certain
304 drugs and chelators [41]. The J-domain is not strictly required for the increased drug sensitivity; however,
305 it is essential for its role as a cochaperone and Rcs activator [13]. DjlA-dependent activation of Rcs
306 signaling requires DnaK and the nucleotide release factor GrpE, but not DnaJ or CbpA [13]. A functional
307 J-domain and the transmembrane helix were both reported to be essential for Rcs induction by DjlA [13,
308 42, 43].

309 As a membrane-anchored cochaperone, it is possible that DjlA directs DnaK to modulate the
310 folding and/or conformation of an Rcs component or the interaction of Rcs components. This is further
311 supported by our observation that DjlA, uniquely, can overcome the tight interaction between IgaA and
312 RcsD T411A (Fig. 3B). Therefore, we tested the effect of DjlA overproduction on the IgaA-RcsD
313 interaction in BACTH assays. We examined the IgaA-RcsD interaction when *djlA* was cloned downstream
314 of IgaA-T18, such that its expression is controlled by the same IPTG-inducible promoter as IgaA. Fig. 5A
315 shows that there is a marked decrease in the IgaA-RcsD interactions when DjlA is overexpressed. To
316 confirm that this effect is due to the cochaperone activity of DjlA, we also tested an inactive DjlA mutant,
317 a H233Q mutation known to be defective for DnaK cochaperone activity [13, 40]. The overexpression of
318 this DjlA H233Q mutant did not disrupt the IgaA-RcsD interaction. Next, we asked if DjlA can weaken the
319 tight interaction between IgaA and the RcsD T411A mutant (Fig. 5B). DjlA overcame this strong interaction
320 and could act even when the periplasmic domain of RcsD was not present (Fig. 5B, T411A Δperi). This

321 contrasts with loss of DsbA, which affected the periplasmic but not the cytoplasmic interactions between
322 IgaA and RcsD (Fig. 4), and is consistent with the ability of overproduced DjlA to cause Rcs induction
323 even when RcsDT411A is present (Fig. 3B). We also tested if any of the other Rcs components are required
324 for DjlA to affect these interactions by carrying out the same assay in derivatives of the BTH101 strain
325 carrying Δ*rcsB* (EAW1), Δ*rcsC* (EAW2), *or* Δ*rcsF* (EAW4) mutants. DjlA was able to weaken the
326 interaction between IgaA and RcsD in the absence of each of these proteins (Fig. 5C). This suggests that
327 DjlA acts directly as a cochaperone, remodeling the RcsD-IgaA interaction with one or both proteins as
328 direct targets for DjlA.

329 Previous studies speculated that RcsC is the target of DjlA likely via transmembrane domain
330 interactions, although that work was done before RcsD and IgaA were known or characterized [42]. As
331 shown above, the periplasmic domain of RcsC was not needed for DjlA induction, but the role of the RcsC
332 transmembrane helices had not been tested. We had previously demonstrated signaling by a $RcsC_{MalF}$ strain
333 containing the RcsC cytoplasmic domain fused to the first two transmembrane (TM) helices of the maltose-
334 transporter membrane protein MalF [9]. $RcsC_{MalF}$ increased the basal Rcs signal of the strain, but it
335 responded to a RcsF-dependent signal like PMBN [9]. DjlA overexpression activated Rcs signaling in this
336 strain, demonstrating that DjlA does not need to interact with the RcsC TM helices (Fig. S5A).

337 We further examined the role of the DjlA TM helix in DjlA-dependent Rcs activation. Point
338 mutants in the TM helix of DjlA have been shown to completely block Rcs activation without affecting its
339 stability or localization [42]. Furthermore, the DjlA TM helix is a dimerization domain and contains
340 conserved glycine residues important for Rcs induction [44]. We replaced the DjlA TM helix with the first
341 two MalF TM helices such that the cytoplasmic portion of DjlA is anchored to the membrane with the MalF
342 helices ($DjlA_{MalF}$; Fig. S5B). We tested P_{rprA}::mCherry induction upon overexpression of this $DjlA_{MalF}$
343 variant in a Δ*djlA* Δ*rcsF* strain. We observed that this chimeric $DjlA_{MalF}$ variant is capable of inducing Rcs
344 signaling, unlike the DjlA H233Q mutant or the DjlA ΔTM variant lacking any TM helix (Fig. S5B). These
345 results lead us to conclude that the DjlA TM helix does not have an active role in Rcs induction, but that

346 membrane localization is indeed essential. Previous reports did not observe any Rcs induction with either
347 DjlA ΔTM or a MalF-DjlA chimeric variant [13, 42, 44]. The discrepancy could be due to the somewhat
348 different $DjlA_{MalF}$ protein construct used by us or may reflect the increased sensitivity of our P_{rprA}::mCherry
349 fluorescent reporter as compared to the *cps-lacZ* beta-galactosidase assay used previously. We further tested
350 the ability of DjlA ΔTM and $DjlA_{MalF}$ to break the IgaA-RcsD interaction using the BACTH assay. Fig.
351 S5C shows that both of these DjlA constructs can disrupt the interaction. This is consistent with the DjlA
352 TM helix not having a specific role in recognizing its Rcs target protein. T18-IgaA levels did not decrease
353 upon overexpression of DjlA (Fig. S5D). Surprisingly, DjlA ΔTM was also capable of disrupting the IgaA-
354 RcsD interactions in BACTH even though it was not functional in Rcs activation. Possibly this is due to
355 the difference in protein levels of IgaA/RcsD/DjlA between these two assays. Thus, the TM helix of DjlA
356 is important for inducing signaling but may be less important for recognizing its Rcs substrate.

357 DjlA was also able to disrupt the interaction of IgaAΔcyt with RcsD (Fig. S5C). We have previously
358 shown that the periplasmic interaction of IgaA and RcsD drives the signal in the BACTH assay [9].
359 Assuming DjlA, with the J-domain in the cytoplasm, interacts with cytoplasmic domains of its substrates,
360 the observation that full-length DjlA can disrupt IgaAΔcyt-RcsD interactions may suggest that DjlA affects
361 interactions of IgaA with the PAS-like domain of RcsD, leading to conformational changes that lessen the
362 strong periplasmic contacts between RcsD and IgaA. Interestingly, the DjlA ΔTM was less effective than
363 full length DjlA in disrupting IgaAΔcyt-RcsD interactions.

364 If multicopy DjlA weakens IgaA-RcsD interactions, it could be speculated that it has a role in
365 modulating these interactions even in single copy under appropriate physiological conditions. However, we
366 failed to find a single copy phenotype of Δ*djlA* for Rcs signaling. A strain devoid of DjlA responded like a
367 wild-type strain to varying doses of PMBN (Fig. S6A) and responded to A22 and mecillinam (Fig. S6B).
368 It also responded similarly even at elevated temperature (42°C) (Fig. S6C). While we were unable to detect
369 a role for single copy DjlA for Rcs induction, BACTH assays of IgaA-RcsD interactions showed a
370 somewhat better interaction in the absence of DjlA, consistent with its proposed role in chaperoning this

371 interaction (Fig. S6D). Consistent with a role for DjlA for the cytoplasmic interaction of these proteins, an
372 increased interaction of RcsD Δperi with IgaA was also seen in the Δ*djlA* strain. RcsD T411A, with a tighter
373 cytoplasmic interaction with IgaA, was unaffected by the absence of DjlA. These results are consistent with
374 the idea that DjlA plays a role in the cytoplasmic signaling interactions of IgaA and RcsD, but under
375 conditions not yet identified.
376
377 **DrpB activates Rcs independently of its cell division role**
378 In contrast with DsbA and DjlA, induction by DrpB overexpression has a requirement for the RcsC
379 periplasmic domain for Rcs activation (Fig. 2). Whether there is a direct interaction between DrpB and
380 RcsC for the signaling to occur or the RcsC periplasmic domain senses a signal generated by DrpB
381 overexpression is not yet known. DrpB is a small (100 aa) protein with two transmembrane helices and a
382 small periplasmic region (see schematic in Fig. S7A). There are no additional recognizable domains.
383 However, DrpB was identified as a multicopy suppressor of the growth defect of a Δ*ftsEX* mutant at low
384 ionic strength [45]. FtsEX is an ABC transporter that coordinates peptidoglycan remodeling and cell
385 division, allowing cell separation. FtsEX helps in recruitment of downstream cell division proteins to the
386 Z-ring, cell constriction, and activation of periplasmic peptidoglycan amidases[46-48]. FtsEX mutants
387 display chaining defects and have low viability in low-osmolarity medium. DrpB localizes to the divisome
388 and overexpression allowed the Δ*ftsEX* [45]. Activation of amidases by FtsEX is not strictly required for
389 survival in low salt medium so it is likely that overproduction of DrpB rescued the growth defect by
390 improving recruitment of downstream components of the divisome [45, 48]. Although no cell division or
391 cell morphology defects were observed in a Δ*drpB* strain, a double deletion strain with another cell-division
392 protein, DedD, was filamentous and DrpB was found to interact with multiple divisome-associated proteins
393 [45].
394 RcsB positively regulates a promoter of *ftsZ*, and multicopy RcsF is a known suppressor of the
395 temperature sensitive *ftsZ84* mutant [3]. Although DrpB did not rescue the *ftsZ(Ts)* phenotype [45], it

396 seemed possible that the ability of DrpB to act as a weak suppressor of the *ftsEX* mutant is due to its role
397 as an Rcs activator. To test this hypothesis, we asked whether RcsB was needed for the ability of DrpB to
398 suppress the growth defect of Δ*ftsEX* cells in the absence of salt. We overexpressed DrpB from a plasmid-
399 encoded arabinose-inducible promoter in Δ*ftsEX* and Δ*ftsEX* Δ*rcsB* strains and assayed colony formation
400 on LB medium with and without NaCl. As seen in Fig. 6A, multicopy DrpB can rescue the growth defect
401 of *ftsEX* mutants even in cells deleted for *rcsB*, demonstrating that the suppression of Δ*ftsEX* is not via Rcs
402 activation. We also asked whether activation of Rcs by DrpB required *ftsEX*, using the P_{rprA}::mCherry
403 reporter in a Δ*ftsEX* strain. We found that DrpB indeed induces Rcs in this strain (Fig. 6B). Therefore, the
404 role of DrpB in cell growth in the absence of Δ*ftsEX* appears to be independent of Rcs activation and vice
405 versa.

406 A set of DrpB mutants were constructed in the pBAD plasmid and tested both for Rcs induction
407 and for ability to rescue the growth of Δ*ftsEX* in the absence of salt (Fig. S7). Since the periplasmic domain
408 of RcsC is needed for DrpB signaling, it could be hypothesized that there is a periplasmic interaction
409 between these proteins. Therefore, we constructed a DrpB mutant with a deletion of its periplasmic region
410 ($\Delta peri_{48-57}$); this deletion had no effect on the ability of DrpB to activate Rcs (Fig. S7A). However, DrpB
411 $\Delta peri_{48-57}$ did not rescue the growth of the Δ*ftsEX* mutant, suggesting it is important for this function (Fig.
412 S7B). An interaction between the transmembrane regions of DrpB and RcsC also seemed possible. Based
413 on the sequence similarity with other DrpB homologs, we generated point mutants in four highly conserved
414 amino acid residues in and around each of the TM helices of DrpB. Fig. S7A shows the effect of these
415 mutants on Rcs signaling in a strain deleted for RcsF. Only DrpB T89A had lost the ability to activate Rcs.
416 This allele only slightly decreased suppression of Δ*ftsEX* (Fig. S7B). The DrpB R38F had decreased but
417 not absent activity for both induction of Rcs and suppression of Δ*ftsEX* (Fig. S7B). We cannot rule out that
418 these mutants are less active due to mislocalization or decreased stability. However, overall the results
419 confirm the existence of two separable functions of DrpB, with the periplasmic region critical for

420 suppression of Δ*ftsEX* but not for Rcs induction, and T89A critical for Rcs induction but reasonably able to
421 suppress Δ*ftsEX*.

422 The BACTH assay was used to test if DrpB directly interacts with any of the Rcs components.
423 However, full-length RcsC has previously been found to be non-functional in the BACTH assay [9], and
424 was also negative for interaction with DrpB (Fig. S8A). We observed variable and weak (not significant)
425 interactions of DrpB with both IgaA and RcsD (Fig. S8A). DrpB interacted with multiple divisome proteins
426 as well as with MalF (used as a control) in a previous study, suggesting the possibility of false-positives in
427 BACTH assays with other membrane proteins [45]

428 As with DjlA, we were not successful in defining an Rcs phenotype for deletion of *drpB*. The Δ*drpB*
429 strain responds to PMBN, A22 and mecillinam (Fig. S8B), which is consistent with a previous observation
430 that DrpB is not needed for the Rcs response to osmotic shock or ethanol stress [15]. Multicopy DrpB also
431 was previously found to induce the *psp* (phage shock) signaling pathway [15]. Rcs induction by DrpB was
432 unaffected by the absence of *psp* components *pspC* and *pspF* (Fig. S8C), ruling out induction of Rcs
433 indirectly via induction of Psp. More studies are needed to ascertain if DrpB activates the Rcs cascade by
434 interacting directly with RcsC and the physiological conditions during which it functions as an Rcs
435 activator.

436 Similar to DrpB, a group of small cytosolic proteins in the *ycgz-ymgABC* operon, which is involved
437 in biofilm formation and acid-resistance, have been demonstrated to trigger the Rcs cascade [17, 49].
438 AriR/YmgB, in complex with YcgZ and YmgA, was reported to targts RcsC to induce the Rcs pathway
439 [50]. We tested the Rcs activation by YmgB in our strains and found it to be RcsF independent and blocked
440 by the RcsD T411A mutation (Fig. S9). However, in contrast with DrpB, it is independent of the periplasmic
441 domain of RcsC, indicating a different mode of Rcs activation.

442

443 **Discussion**

444 The Rcs phosphorelay is a remarkably sophisticated signaling pathway capable of responding to a
445 wide array of stress signals at the cell envelope. RcsF plays a vital role in sensing most of the Rcs induction
446 cues but is not strictly necessary for activating signaling. Our study elucidates diverse modes of activation
447 of the Rcs phosphorelay which are independent of RcsF (Fig 7). The results demonstrate that RcsF is not
448 the sole sensor for this pathway. In particular, our identification of DrpB as an RcsF-independent activator
449 suggests the possibility of other yet unidentified RcsF-independent activators and particularly activators
450 that act via the RcsC periplasmic domain.

451 We delineate how three RcsF-independent activators trigger the Rcs phosphorelay, each in a
452 different fashion. Our current understanding of the regulation of Rcs signaling is primarily based on the
453 interactions of IgaA with RcsF and RcsD. Interactions of RcsF with IgaA form the first level of regulation
454 crucial for activation of signaling (Fig. 1A). Signals detected by RcsF change the interaction of IgaA with
455 RcsD; this IgaA-RcsD interaction serves as the regulatory switch necessary for signal activation. Dependent
456 on the nature of these interactions, the RcsC histidine kinase acts as either a phosphatase (RcsB response
457 regulator not phosphorylated, inactive) or a kinase (RcsB response regulator phosphorylated and active).
458 The IgaA-RcsD interactions are also essential for repression of signaling, thereby preventing constitutive
459 activation and the resulting lethality. Our work underscores the importance of these IgaA-RcsD interactions
460 in regulating this cascade even in the absence of RcsF-dependent activation. Signaling in all three cases, in
461 cells deleted for DsbA or overproducing DjlA or DrpB, is dependent on RcsC and RcsD and does not
462 initiate signaling merely by increasing expression of components such as RcsB.

463

464 **Interrupting the interactions of RcsD and IgaA induce Rcs signalling**

465 Loss of DsbA or DjlA overproduction each activate signaling by weakening the interactions
466 between IgaA and RcsD, affecting their folding/conformation via distinct modes. We have previously
467 shown that IgaA and RcsD interact both through their periplasmic domains and their cytoplasmic domains
468 ([9], Fig. 1A). The periplasmic strong contact provides an anchor that keeps signaling from rising too high.
469 Based on the identification of the RcsDT411A mutant in the cytoplasmic PAS domain of RcsD that blocks

470 RcsF-dependent induction, the cytoplasmic contact was defined as the regulatory switch region. The loss
471 of DsbA impacts the periplasmic contacts, likely due to its role in formation of disulfide bonds in IgaA, and
472 therefore IgaA folding. This is reflected in a decrease in the interaction of IgaA and RcsD in the absence of
473 DsbA and in elevated Rcs signaling, further increased when cells are treated with DTT. Presumably in a
474 strain devoid of DsbA, a fraction of IgaA is in a reduced state with one or both disulfide bonds disrupted;
475 addition of DTT leads to the disruption of any remaining disulfide bonds. Mutating the IgaA periplasmic
476 cysteines predicted to be involved in these disulfide bonds mimics the *dsbA* mutant, decreasing the
477 interaction of IgaA and RcsD (Fig. S4C) and increasing signaling. RcsF itself requires disulfide bonds for
478 proper folding and function [30, 31]. Therefore, it is not surprising that *dsbA* mutants no longer recognize
479 RcsF-dependent cues such as A22 and mecillinam (Fig. S4A), since RcsF is non-functional in this strain.
480 Similar observations have been made in *Salmonella*; *Salmonella dsbA* mutants activate Rcs, independent
481 of RcsF, and this is increased upon DTT addition, while a strain carrying a *bamB* deletion induces Rcs,
482 dependent upon RcsF and is unaffected by DTT treatment [51].

483 We might have also expected PMBN, which normally induces the Rcs system in an RcsF-
484 dependent fashion (see Fig. 1B) to be ineffective in the *dsbA* mutant. However, it induces in much the
485 manner that DTT does, independently of *rcsF* (Fig. 1B). This result suggests that PMBN causes some redox
486 stress, in addition to the LPS/membrane damage that leads to RcsF-dependent induction. When the Dsb
487 network is functional, DTT cannot induce Rcs signaling and any PMBN induction requires RcsF,
488 suggesting that Rcs probably does not monitor disulfide bond formation in the periplasm as part of its
489 normal function. Instead, the disulfide bonds are necessary for proper folding of IgaA to allow the
490 periplasmic interaction with RcsD. We cannot rule out the possibility that under extreme oxidative stress,
491 IgaA disulfide bonds might be disrupted sufficiently to induce Rcs signaling. A study of the roles of the
492 periplasmic cysteines of IgaA in *Salmonella* also found that disulfide bonds were critical both for proper
493 repression of Rcs and, to some extent, for viability of the cells [33].

494 Overproduction of DjlA, a membrane-localized DnaJ family protein, also loosens the interaction
495 of IgaA and RcsD (Fig. 5A) and turns up signaling independently of RcsF (Fig. 1B); these effects depend

496 on an active J domain (mutated in DjlA H233Q). However, in this case, the primary effect is likely on the
497 cytoplasmic domains of IgaA, RcsD, or both of these proteins. This is suggested both by the observation
498 that DjlA overproduction but not loss of DsbA overcomes the RcsD T411A mutation (Fig. 3) and by the
499 location of the J domain in the cytoplasm. The ability of DjlA overproduction to induce signaling also
500 allows us to conclude that the interaction of the RcsD PAS-like domain with the IgaA cytoplasmic domain
501 can regulate activation by both RcsF-dependent and RcsF-independent signals.

502 DjlA was the only RcsF-independent activator which overcame the heightened interaction between
503 RcsD T411A mutant and IgaA. This would be consistent with DjlA acting as a chaperone to mediate these
504 interactions. Molecular chaperone systems can assist protein-protein interactions by loosening and altering
505 protein conformations. Unlike DnaJ and CbpA, the other *E. coli* DnaJ family proteins capable of working
506 with DnaK, DjlA does not carry a specific substrate-binding domain, so it is not known how it identifies its
507 clients [42]. Since only DjlA, and not the other two DnaJ family proteins, induces Rcs, it seemed possible
508 that the membrane insertion of DjlA is critical in recruiting DnaK to the sites of IgaA/RcsD. The
509 transmembrane helix of DjlA contains several conserved residues and it has been postulated earlier that this
510 helix helps in substrate interaction [42]. This notion is reinforced by the lack of signaling from a cytosolic
511 soluble form of DjlA ([13, 42], Fig. S5B). The transmembrane helix is also a dimerization helix, and DjlA
512 fused to any other transmembrane helix was previously found to be incapable of activating this system [44].
513 However, we found that DjlA fused to the MalF transmembrane domains can activate Rcs, strongly
514 suggesting this helix is not required for Rcs interaction. Our results also rule out RcsC as the DjlA substrate
515 for Rcs activation. Either IgaA or RcsD, or the complex could be a target of DjlA; however, the ability of
516 DjlA to disrupt interaction of IgaAΔcyt and RcsD (Fig. S5C) is most consistent with RcsD as the target.
517 Because the periplasmic interaction of RcsD and IgaA is sufficient for a strong interaction signal in the
518 BACTH assay, we can also conclude that the action of DjlA on the cytoplasmic domain of RcsD must lead
519 to a change in the RcsD periplasmic domain.

520 The effects here were seen when DjlA was overproduced. We do not know whether or when the
521 chromosomally encoded DjlA is able to modulate the IgaA-RcsD interaction. Deletion of *djlA* strengthened

522 the interaction of IgaA and RcsD in the BACTH assay (Fig. S6D) but did not have any effect on Rcs
523 induction under a variety of conditions (Fig. S6). Not much is known about the physiological signals
524 regulating DjlA expression; DjlA-stimulation of Rcs might be relevant under specific growth conditions or
525 might be important for particular inducing signals not tested here. There is also evidence that DjlA acts as
526 a negative regulator of Rcs [5, 52]. Those studies demonstrated a stimulation of the Rcs signal upon deletion
527 of DjlA, particularly in mutant strains such as *mdo* and *rfa* which are already activated for Rcs in an RcsF-
528 dependent manner. Lack of DjlA could increase the envelope stress caused by mutants in *mdo* and *rfa*
529 independently of the RcsF-independent effect seen here. Undoubtedly, DjlA has substrates other than the
530 Rcs system, and possibly the opposing effects (controlling envelope stress to negatively regulate Rcs and
531 overcoming the RcsD/IgaA protein to induce Rcs) balance each other, making it more difficult to define a
532 single copy effect.
533
534 **Rcs Activation via Histidine Kinase RcsC**
535 Uniquely among the three proteins we investigated, DrpB required the RcsC periplasmic domain
536 for signaling. RcsC is a member of a broad family of histidine kinases; in many of these, the periplasmic
537 domains are critical for sensing environmental signals and regulating histidine kinase activity [53-55]. In
538 our previous work, we found that IgaA interacted with RcsD, the phosphorelay protein, rather than RcsC
539 and Rcs inducing treatments were independent of the RcsC periplasmic domain [9]. Thus, while RcsC
540 activity (kinase vs. phosphatase) must be adjusted by RcsF-dependent induction, there was no evidence for
541 a role of RscC in signal sensing. Thus, the identification of DrpB and its dependence on the RcsC
542 periplasmic region demonstrates the likelihood that some signals act in the "classical" way seen for other
543 histidine kinases; if so, such signals would be independent of RcsF. While we do not know if DrpB acts
544 directly or indirectly on RcsC, it is tempting to speculate that the RcsC periplasmic domain is sensing a
545 signal created byDrpB overexpression, allowing RcsC to activate signaling. Interestingly, a ribosome
546 profiling study revealed DrpB as one of the proteins upregulated during severe acid stress in *E. coli* and this
547 may be linked to its Rcs function [56]. Alternatively, the overproduction of DrpB itself is a source of stress

548 which is detected by RcsC. DrpB overproduction also leads to the induction of another envelope stress
549 response, the Psp response pathway [15]. The Psp response primarily detects and mitigates stress at the
550 inner membrane (reviewed in [57]). While we find that the Psp pathway is not necessary for Rcs induction
551 by DrpB (Fig. S8), it will be of interest to see whether other inducing signals, shared by these two systems,
552 also share dependence upon the RcsC periplasmic domain.

553 Further evidence for RcsC as a sensor comes from studies on the protein YmgB. YmgB is a
554 cytoplasmic protein involved in biofilm formation and acid-resistance and it stimulates the Rcs pathway,
555 reportedly by interacting with the RcsC cytoplasmic domain [49, 50]. In our hands, and consistent with the
556 model suggested by DrpB overexpression, YmgB-dependent induction is RcsF-independent, but, unlike
557 DrpB, is also independent of the periplasmic domain of RcsC (Fig. S9). This is consistent with previous
558 work on YmgB and raises the possibility that RcsC in fact senses different signals with its cytoplasmic and
559 periplasmic domains.

560 A number of other proteins have been found to affect Rcs activity. YpdI, a lipoprotein of unknown
561 function, induces mucoidy in the absence of RcsF [16]. Activation of Rcs in a double mutant of *yqjA* and
562 *yghB*, both membrane proteins and putative lipid flippases, is partially dependent on RcsF [20, 58].
563 Deciphering their mechanisms could add to our knowledge about Rcs regulation.

564 Overall, our results emphasize the versatility and flexibility of the Rcs pathway. RcsF senses stress
565 at the outer cell surface and in the periplasm. The RcsF-independent signaling pathways studied here
566 suggest that, in addition, RcsC may play a role in sensing stressors at the cytoplasmic membrane, and
567 possibly in the cytoplasm as well. Possibly this sensing by RcsC represents the remnants of the original
568 version of this system, before RcsD, IgaA and RcsF evolved to sense a broader set of inducing signals.
569 Clearly there is still much to be learned about this system, across species, and in different natural
570 environments. Structural information on the Rcs proteins and how they interact is also still lacking. We
571 look forward to better understanding this unique system in the future.

572

573 **Materials and Methods:**

574

575 **Bacterial growth conditions and strain construction:**

576 The strains were grown in LB medium with appropriate antibiotics (ampicillin 100 μg/ml, kanamycin 30-
577 50 μg/ml, chloramphenicol 10 μg/ml for *cat-sacB* allele or 25 μg/ml for chl^R plasmids, tetracycline 25μg/ml,
578 zeocin 50μg/ml). Glucose at a final concentration of 1% was added to reduce the basal expression from the
579 plasmids containing pBAD and pLac promoters.

580 Strains, plasmids, primers and synthetic DNA fragments (gBlocks) used in this study are listed in
581 Tables S1, S2, S3, and S4 respectively. Oligonucleotides and gBlocks were from IDT DNA, Coralville, IA.
582 Strains were constructed by recombineering or P1 transduction with selectable markers (Table S1).
583 Recombineering was done in strains carrying a chromosomal mini-λ Red system (*miniλ::tet*) or a plasmid-
584 borne Red system (pSIM27). Some strains were generated by direct P1 transduction from the corresponding
585 mutant strains in the Keio collection [59]. Plasmids were constructed by the Gibson assembly method using
586 the In-fusion HD Cloning kit (Takara Bio USA) [60]. PCR products were purified using column purification
587 (Qiagen) and transformed into NEB DH5α F'*lacIQ* cells. Site-directed mutagenesis in the genes was carried
588 out using the QuikChange Site-directed mutagenesis kit (Agilent). Sequencing was done to confirm the
589 chromosomal and plasmid modifications.

590

591 **Screening for multicopy RcsF-independent activators**

592 A pBR-based plasmid library [61] was transformed into EAW34 electrocompetent cells. Aliquots of the
593 transformed mixture were plated on LB plates containing 100 μg/ml ampicillin and incubated overnight at
594 37°C. Subsequently, the plates were imaged and the colonies displaying high fluorescence were restreaked
595 on LB ampicillin plates and purified. The plasmid DNA was isolated from these colonies and retransformed
596 into EAW34 to validate their phenotype. The positive candidate plasmids were isolated, sequenced and the
597 reads mapped to the *E. coli K-12 MG1655* genome to identify the inserts.

598

599 **Fluorescence reporter assays:**

600 Growth and fluorescence assays for Rcs activation were carried out in 96-well plates in a Tecan Spark
601 microplate reader. All the strains carried a P_{rprA}::mCherry transcriptional fusion at the *ara* locus as a reporter
602 for Rcs signaling [9]. For strains carrying overexpression plasmids expressing DjlA, DrpB, or RcsF, the
603 overnight cultures were grown in MOPS minimal glucose (0.2%) medium (Teknova). For the
604 P_{rprA}::mCherry assays for these strains, they were diluted to OD_{600} 0.03-0.05 in MOPS minimal glycerol
605 media (0.05% glucose, 0.5% glycerol) with 0.02% arabinose (induced) or 0.2% glucose as an uninduced
606 control. Both the optical density (OD_{600}) and mCherry fluorescence were monitored every fifteen minutes
607 for 12 hours. Polymyxin B nonapeptide (PMBN; Sigma) was used at 20 µg/ml, to induce the Rcs system.
608 A22 (an MreB inhibitor) was used at 5 µg/ml, and mecillinam was used at 0.3 µg/ml. Each assay was
609 performed in technical duplicates in the microtiter plate, with the biological replicates performed on
610 different days. The fluorescence values at equivalent OD_{600} values (0.4 ± 0.04) for each strain were
611 converted to bar graphs and plotted as signal fold change of fluorescence signal over the uninduced wild
612 type strain. Error bars represent the standard deviation of at least 3 assays. For strains that did not reach an
613 OD_{600} value of 0.4, the OD is noted on the bar graph. For the P_{rprA}::mCherry assays for the strains not
614 carrying any plasmids, MOPS minimal glucose media was used for growing overnight cultures and
615 performing the fluorescence assays. For the assays pertaining to *dsbA* mutants, the overnight cultures were
616 grown in LB medium. Subsequently, cells were washed with and diluted to OD_{600} 0.05 in MOPS minimal
617 glucose media to carry out the P_{rprA}::mCherry assay. To activate the Rcs system, Dithiothreitol (DTT,
618 Sigma) was added at a final concentration of 1mM or Polymyxin B nonapeptide (PMBN; Sigma), was used
619 at 20 µg/ml. All assays were performed at 37°C, unless otherwise indicated. Values derived from at least
620 three independent experiments were plotted to show the mean with error bars indicating standard deviation.
621 These were statistically analyzed by multiple unpaired *t*-tests using GraphPad Prism 10 software.

622

623 **Bacterial adenylate cyclase two hybrid assay (BACTH):**

624 For the bacterial adenylate cyclase two hybrid assay (BACTH), an adenylate cyclase mutant strain
625 (BTH101) or a derivative if this strain was used. The proteins whose interactions were being examined
626 were cloned into the T18 and T25 portions of adenylate cyclase [34, 35]. The reconstitution of adenylate
627 cyclase upon their interaction allows production of cAMP, which interacts with CRP to activate the *lac*
628 operon, assayed as beta-galactosidase activity. In the absence of interaction, T18 and T25 do not get
629 reconstituted to form a functional adenylate cyclase and the strain does not express beta-galactosidase. The
630 proteins used in this study were fused at their C-terminal to the Cya fragments. Plasmids expressing IgaA
631 or RcsD as T18/T25 fusion constructs were cotransformed into BTH101, plated on LB-agar medium
632 containing 100 µg/ml ampicillin and 50 µg/ml kanamycin and incubated at 30°C for 2 days. To measure
633 the beta-galactosidase activity, the resulting colonies were inoculated and grown overnight in LB medium
634 containing 100 µg/ml ampicillin, 50 µg/ml kanamycin, and 0.5 mM IPTG at 30°C. The beta-galactosidase
635 assay was performed in 96-well plates. The activity was analysed by measuring the kinetics of ONPG
636 degradation by monitoring the OD 420 nm at 28°C for 40 min at intervals of 1 min in a Tecan Spark
637 microplate reader. The beta-galactosidase activity was calculated using the slope of OD 420 divided by
638 their OD 600. Each protein fusion paired with the cognate vector produces very little activity and these
639 were used as negative controls. Every graph is compiled from at least 3 separate sets of assays, and the
640 beta-galactosidase activity is plotted relative to the IgaA/RcsD interaction in that particular experiment.
641 To test the effect of DsbA activity on the various IgaA/RcsD constructs, the BACTH assays were
642 carried out in BTH101 and a *dsbA* mutant derivative of BTH101 (AP58). To test the effect of DjlA on the
643 IgaA/RcsD interactions, d*jlA* or mutants of *djlA* were cloned downstream of IgaA under the control of the
644 same promoter. The assay was carried out in BTH101 or its derivatives EAW1, EAW2, and EAW4 as
645 above and interactions plotted relative to the IgaA/RcsD interaction in WT, set to 1.
646
647 **Western blots**

648 For Fig. S4D, plasmids were transformed into EAW8 and EAW62 and for Fig. S5D, the plasmids were
649 transformed into *E. coli* DH5α competent cells (NEB). The colonies were inoculated into LB media
650 containing Amp (100 µg/ml) and 1 mM IPTG and then grown for 8 hours at 30°C. One ml of culture was
651 precipitated using TCA, washed in acetone and resuspended in LDS sample buffer standardized to OD. 8
652 µl volumes were loaded on 4–12% NuPage gradient gels (Invitrogen, CA) and then transferred onto
653 nitrocellulose membranes in an iBlot2 transfer device as per manufacturer's specifications (Invitrogen,
654 CA). The membranes were blocked with Casein PBS and then incubated in CyaA-T18 mouse monoclonal
655 primary antibody at 1:10,000 (Santa Cruz Biotechnology, CA) or/and a mouse monoclonal anti-EF-Tu at
656 1:10,000 (Hycult Biotech, PA) overnight at 4°C. Secondary fluorescent antibody anti-mouse DyLight800
657 (Bio-Rad, CA) was used at 1:10,000. Imaging was done on a ChemiDoc MP imaging system (Bio-Rad).
658
659 **Viability testing of *ftsEX* mutants:**
660 The wildtype and *ftsEX* deletion strains were transformed with the pBAD33 vector or a DrpB containing
661 plasmid and plated on LB Miller-agar medium at 30°C containing 25 µg/ml chloramphenicol. Overnight
662 cultures were grown in LB Miller medium 25 µg/ml chloramphenicol at 30°C. Cells were harvested from
663 1 mL of culture and diluted to OD_{600} 1.0 in LB Miller or LB0N (LB without any NaCl) medium. Serial
664 dilutions (10-fold) were made and 4 µl was spotted onto LB Miller-agar or LB0N-agar plates containing 25
665 µg/ml chloramphenicol. Arabinose was added at 0.2% for induction in LB0N. Plates were imaged after 16
666 h of growth at 37°C.
667
668
669

670 **Supplementary tables (S1-S4)**

671 **Table S1: List of strains used in this study.**

672 **Table S2: List of plasmids used in this study.**

673 **Table S3: List of primers used in this study.**

674 **Table S4: List of gBlocks used in this study.**

675

676 **Supplementary figures (Fig. S1-S9)**

677

678 **Acknowledgements:** This research was supported by the Intramural Research Program of the NIH,
679 National Cancer Institute, Center for Cancer Research. We thank members of the Gottesman lab for
680 comments on the manuscript. EAW was supported by a Fi2 PRAT fellowship award from NIGMS. Tae
681 Yoon Chang, a summer student, performed the initial library screen for RcsF-independent Rcs activation
682 that identified DrpB as an activator. We thank David Weiss for discussions and for providing strains (see
683 Table S1).

684

685

686

687

688

689

690 **Figure legends:**

691

692 **Fig. 1: RcsF-independent activators of Rcs signaling. A. Components of the Rcs phosphorelay:** The
693 Rcs pathway is comprised of the hybrid histidine kinase RcsC, the phosphotransferase RcsD, and the
694 response regulator RcsB as well as the upstream regulatory components RcsF and IgaA. Under non-
695 inducing growth conditions, IgaA represses signaling by interacting with RcsD. RcsF senses damage to the
696 envelope and triggers the RcsC-RcsD-RcsB phosphorelay by interacting with IgaA, altering its interaction
697 with RcsD. **B. Rcs activation by overexpression of DjlA and DrpB:** All strains carry a *rprA* promoter
698 fusion to mCherry (P_{rprA}::mCherry); mCherry fluorescence acts as an indicator for Rcs activation. For the
699 P_{rprA}::mCherry assay, the strains overexpressing DjlA (pBAD-DjlA/pPSG961) or DrpB (pBAD-
700 DrpB/pDSW1977) were grown in MOPS minimal glycerol medium containing chloramphenicol (25 µg/ml)
701 and either 0.2% glucose or 0.02% arabinose at 37°C. The RFU at OD 0.4 compared to the uninduced vector
702 control (set to 1) is plotted. The strains used are: WT (EAW8), *rcsF::kan* (AP51), and *rcsB::kan* (EAW31).
703 **C. Rcs signaling in *dsbA* mutants:** For the P_{rprA}::mCherry assay, the cells were grown in MOPS minimal
704 glucose medium at 37°C. The RFU at OD 0.4 as compared to WT uninduced, set to 1, is depicted here. The
705 cells were treated with either 1mM DTT (blue bars) or 20µg/ml PMBN (brown bars) from the beginning
706 of growth. The strains used were: WT (EAW8), *rcsF::cat* (EAW32), *rcsB::kan* (EAW31), *dsbA::kan*
707 (EAW62), *dsbA::kan rcsF::cat* (EAW67), and Δ*dsbA rcsB::kan* (AP12). Details of the assay are described
708 in Materials and Methods. Data from three independent experiments is plotted as mean with error bars
709 indicating the standard deviation. Values were statistically analyzed using multiple unpaired *t*-tests.
710 Statistical significance is indicated as follows: ns ($P > 0.05$; non- significant), * ($P < 0.05$), ** ($P \leq 0.01$),
711 *** ($P \leq 0.001$), and **** ($P \leq 0.0001$).

712

713 **Fig. 2: Requirement of RcsC periplasmic domain for RcsF-independent signaling by DrpB. A. *dsbA***
714 **mutants do not need the RcsC periplasmic domain for signaling:** For the P_{rprA}::mCherry assay, the cells

715 were grown in MOPS minimal glucose medium at 37°C. The RFU at OD 0.4 as compared to WT uninduced,
716 set to 1, is depicted here. The cells were treated with either 1mM DTT or 20µg/ml PMBN. **B. DrpB, but**
717 **not DjlA, requires the RcsC periplasmic domain for Rcs activation:** For the P_{rprA}::mCherry assay, the
718 strains overexpressing DjlA (pBAD-DjlA/pPSG961) or DrpB (pBAD-DrpB/pDSW1977) were grown in
719 MOPS minimal glycerol medium containing chloramphenicol (25 µg/ml) and either 0.2% glucose (-Ara)
720 or 0.02% arabinose at 37°C. The RFU at OD 0.4 compared to the uninduced vector control is plotted. The
721 strains used were: WT (EAW8), *dsbA::kan* (EAW62), *rcsC::tet* (EAW18),), *rcsC::tet dsbA::kan*
722 (EAW63), *rcsC* Δ*peri* (EAW70), and *dsbA::kan rcsC* Δ*peri* (EAW74). Values (mean ± SD) were
723 statistically analyzed using multiple unpaired *t*-tests. Statistical significance is shown as: ns ($P > 0.05$; non-
724 significant), ** ($P \leq 0.01$), and **** ($P \leq 0.0001$).
725
726 **Fig. 3: Effect of RcsD T411A mutation on RcsF-independent signaling. A. RcsD T411A mutation**
727 **blocks signaling by *dsbA*:** For the P_{rprA}::mCherry assay, the cells were grown in MOPS minimal glucose
728 medium at 37°C. The RFU at OD 0.4 as compared to the uninduced WT control, set to 1, is depicted here.
729 The cells were treated with either 1mM DTT or 20µg/ml PMBN. Details of the assay are described in
730 Materials and Methods**. B. DjlA, but not DrpB, can overcome the RcsD T411A mutation for Rcs**
731 **activation:** For the P_{rprA}::mCherry assay, the strains overexpressing DjlA (pDjlA/pPSG961) or DrpB
732 (pDrpB/pDSW1977) were grown in MOPS minimal glycerol medium containing chloramphenicol (25
733 µg/ml) and either 0.2% glucose or 0.02% arabinose at 37°C. The RFU at OD 0.4 compared to the vector
734 uninduced control, set to 1, is plotted. The strains used were: WT (EAW8), *dsbA::kan* (EAW62), Δ*rcsD*
735 (EAW19), Δ*dsbA rcsD541::kan* (AP13), *rcsD T411A* (EAW121), and *rcsD T411A dsbA::kan* (AP14).
736 Statistical significance was calculated using multiple unpaired *t*-tests and is shown as follows: ns ($P > 0.05$;
737 non- significant), * ($P < 0.05$), ** ($P \leq 0.01$), and **** ($P \leq 0.0001$).
738

739 **Fig. 4: DsbA is needed for efficient IgaA-RcsD periplasmic interactions. A. IgaA-RcsD interactions**
740 **are weakened in Δ*dsbA*.** Beta-galactosidase activity was measured in a Δ*cyaA* strain (BTH101 or AP 58
741 (BTH101 Δ*dsbA*)) expressing two plasmids encoding the T18 and T25 domains of adenylate cyclase fused
742 to the proteins of interest and the expression measured compared to vector background. The IgaA/RcsD
743 protein fusion plasmids paired with their cognate vector had very low activity; the three controls were
744 averaged and used as "background" for normalization. The IgaA-RcsD interaction was normalized to 1 and
745 other interactions were plotted relative to this interaction in WT. This data is compiled from separate sets
746 of assays, each normalized relative to the IgaA/RcsD signal in that experiment. The P values are relative to
747 the $dsbA^+$ values. **B. Periplasmic interactions are affected in Δ*dsbA* and a T411A mutation strengthens**
748 **this IgaA interaction.** IgaA and RcsD/T411A were fused to the T18 and T25 domains, respectively. The
749 IgaA-RcsD interaction in WT was normalized to 1 and all other interactions are plotted relative to this
750 interaction. The RcsD T411A mutation tightens the IgaA-RcsD interaction in WT as well as Δ*dsbA*. The
751 plasmids used were pEAW1 (IgaA-T18), pEAW8 (RcsD-T25), pEAW2 (IgaA-T25), pEAW7 (RcsD-T18),
752 pAP101 (IgaA Δcyt), pEAW1peri (IgaA Δperi), and pEAW8T (RcsD T411A-T25). Values (mean ± SD)
753 from independent experiments were statistically analyzed using multiple unpaired *t*-tests. Statistical
754 significance is shown as follows:ns ($P > 0.05$; non- significant), *** ($P \leq 0.001$), and **** ($P \leq 0.0001$).
755
756
757 **Fig. 5: DjlA weakens IgaA-RcsD interactions. A. DjlA loosens IgaA-RcsD interactions:** Beta-
758 galactosidase activity was measured in a Δ*cyaA* strain (BTH101) in the presence of the indicated plasmids.
759 IgaA and RcsD/RcsD T411A were fused to the T18 and T25 domains, respectively. DjlA or the H233Q
760 mutant of DjlA, inactive as a co-chaperone, was cloned downstream of IgaA under the same promoter
761 control. The IgaA-RcsD interaction was normalized to 1 and all other interactions are plotted relative to
762 this interaction. **B. DjlA can disrupt cytoplasmic interactions of IgaA and RcsD:** The IgaA-RcsD
763 interaction was normalized to 1 and all other interactions are plotted relative to this interaction**. C. RcsB,**

764 **RcsC, RcsF are not needed for DjlA to weaken interactions.** The IgaA-RcsD interaction was tested in
765 BTH101 (WT), EAW 1 (*BTH 101 rcsB::tet*), EAW2 (*BTH 101 rcsC::tet*) and EAW4 (*BTH 101 rcsF::cat*).
766 Plasmids used in this set of experiments were pEAW1 (IgaA-T18), pEAW8 (RcsD-T25), pEAW8T (RcsD
767 T411A-T25), pAP804 (RcsD T411A Δperi -T25), pAP1401 (IgaA-T18 + DjlA), and pAP1402 (IgaA-T18
768 + DjlA H233Q). Statistical significance was calculated using multiple unpaired *t*-tests and is shown as
769 follows: ** ($P \leq 0.01$), *** ($P \leq 0.001$), and **** ($P \leq 0.0001$).
770
771 **Fig. 6: DrpB signaling is independent of *ftsEX*. A. Role of DrpB as a *ftsEX* suppressor is independent**
772 **of its role as an Rcs activator:** Strains transformed with the pBAD33 vector or pDrpB (pDSW1977) were
773 grown overnight in LB Miller media with chloramphenicol at 37°C. The cultures were diluted to an OD_{600}
774 of 1 and 4 ul dilutions were spotted on LB Miller (permissive), LB without NaCl, and LB with 0.2%
775 arabinose with no NaCl. All plates contained chloramphenicol (25 µg/ml). Plates were imaged after 16h
776 incubation at 37°C. The strains used are: WT (EC251), *rcsB::kan* (AP158, Δ*rcsB*), Δ*ftsEX* (EC1215), and
777 Δ*ftsEX rcsB::kan* (AP159, Δ*ftsEX* Δ*rcsB*). **B. DrpB can activate Rcs signaling in Δ*ftsEX*:** For the
778 P_{rprA}::mCherry assay, the WT (EAW8) and *ftsE::kan* (AP154, Δ*ftsEX*) strains transformed with the
779 pBAD33 vector or pDrpB (pDSW1977) were grown in MOPS minimal glycerol medium (with 150 mM
780 NaCl) containing chloramphenicol and either 0.2% glucose or 0.02% arabinose at 37°C. The RFU at OD
781 0.4 is plotted relative to uninduced WT with the vector, set to 1. Statistical significance was calculated using
782 multiple unpaired *t*-tests and is shown as follows: ns ($P > 0.05$; non- significant),** ($P \leq 0.01$), *** ($P \leq$
783 0.001).
784
785
786 **Fig. 7: Diverse modes of RcsF-independent activation by DsbA, DjlA, and DrpB.** First, *dsbA* mutants
787 activate Rcs signaling in response to DTT and PMBN. The absence of DsbA likely leads to defective
788 disulfide bond formation and misfolding of the IgaA periplasmic domain. Thus, DsbA is needed to maintain

789 proper IgaA-RcsD interactions in the periplasm and in its absence, IgaA cannot effectively regulate Rcs
790 signaling. Second, DjlA acts as a cochaperone for IgaA-RcsD interactions. Overexpression of DjlA
791 weakens the IgaA-RcsD interactions in the cytoplasm leading to Rcs activation. Third, DrpB
792 overexpression induces the Rcs cascade but it does not act directly on IgaA-RcsD interactions like DsbA
793 and DjlA. Uniquely, DrpB requires the RcsC periplasmic domain to activate Rcs signaling and either
794 activates it by direct interaction with RcsC or via an indirect mechanism involving RcsC as the sensor
795 instead of RcsF.
796
797
798
799
800
801
802
803
804
805
806
807
808
809
810
811
812 **Fig. 1:**

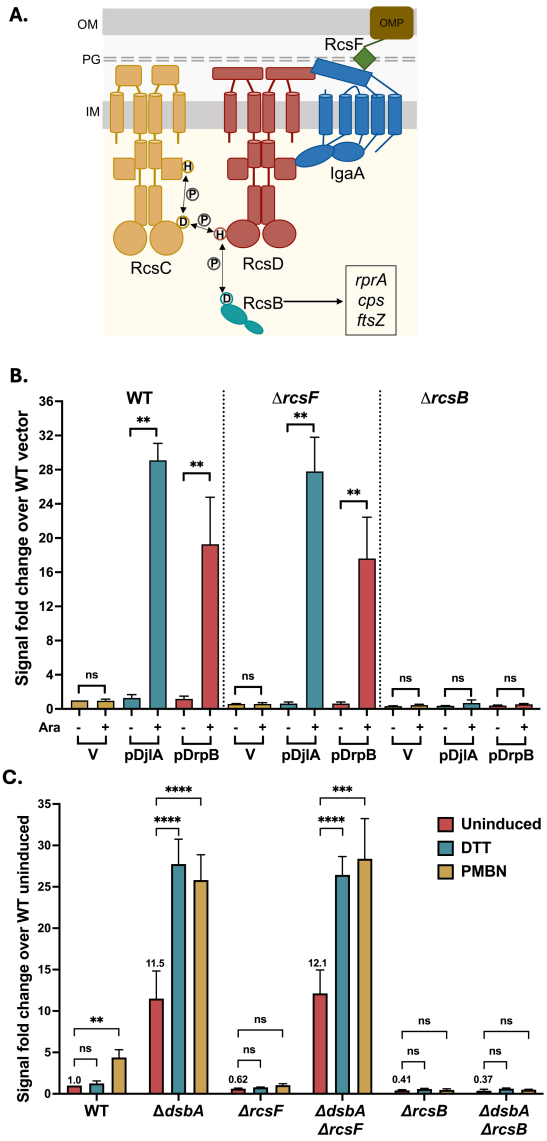
A.
OM
PG
IM
OMP
RcsF
IgaA
RcsC
RcsD
RcsB
rprA
cps
ftsZ
B.
WT
ΔrcsF
ΔrcsB
Signal fold change over WT vector
Ara
V
pDjlA
pDrpB
C.
Signal fold change over WT uninduced
Uninduced
DTT
PMBN
WT
ΔdsbA
ΔrcsF
ΔdsbA ΔrcsF
ΔrcsB
ΔdsbA ΔrcsB

Fig. 2:

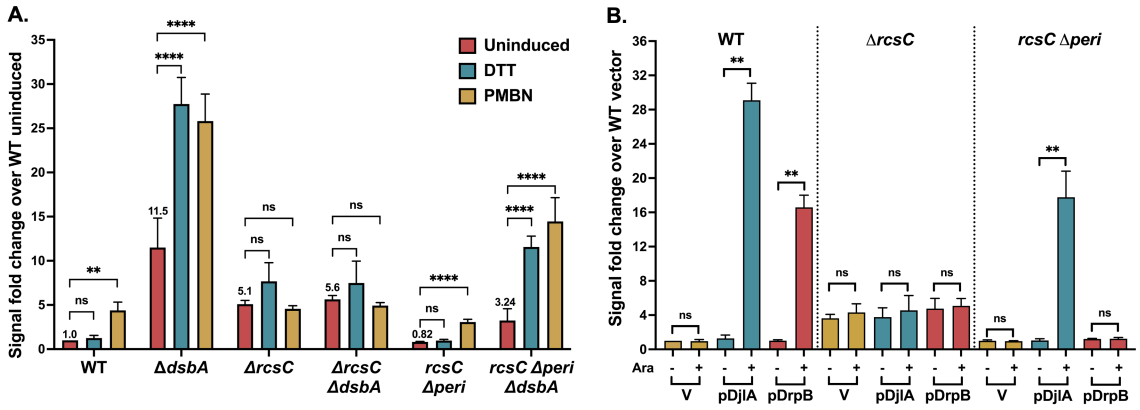
A.
Signal fold change over WT uninduced
Uninduced
DTT
PMBN
WT
ΔdsbA
ΔrcsC
ΔrcsC ΔdsbA
rcsC Δperi
rcsC Δperi ΔdsbA
B.
Signal fold change over WT vector
WT
ΔrcsC
rcsC Δperi
Ara
V
pDjlA
pDrpB

Fig. 3:

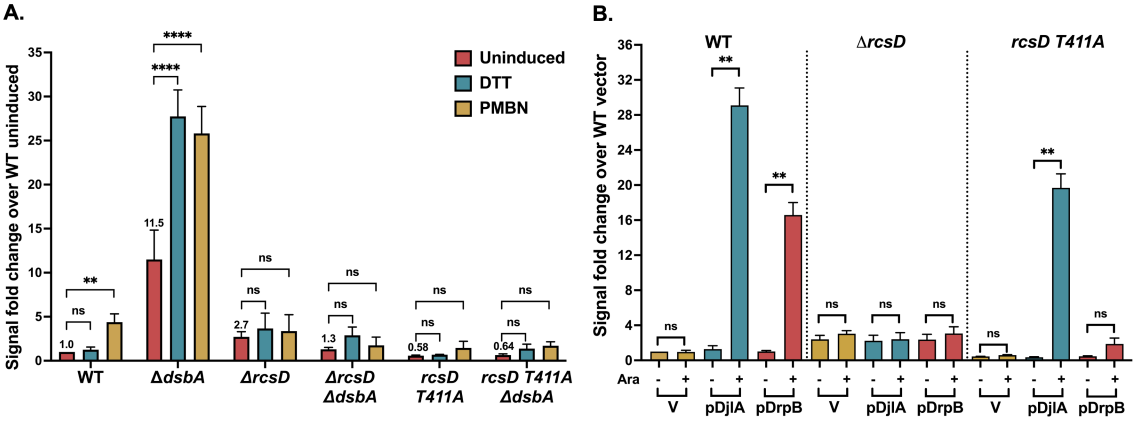
A.
Signal fold change over WT uninduced
Uninduced
DTT
PMBN
WT
ΔdsbA
ΔrcsD
ΔrcsD ΔdsbA
rcsD T411A
rcsD T411A ΔdsbA
B.
Signal fold change over WT vector
WT
ΔrcsD
rcsD T411A
Ara
V
pDjlA
pDrpB

857 **Fig.4:**

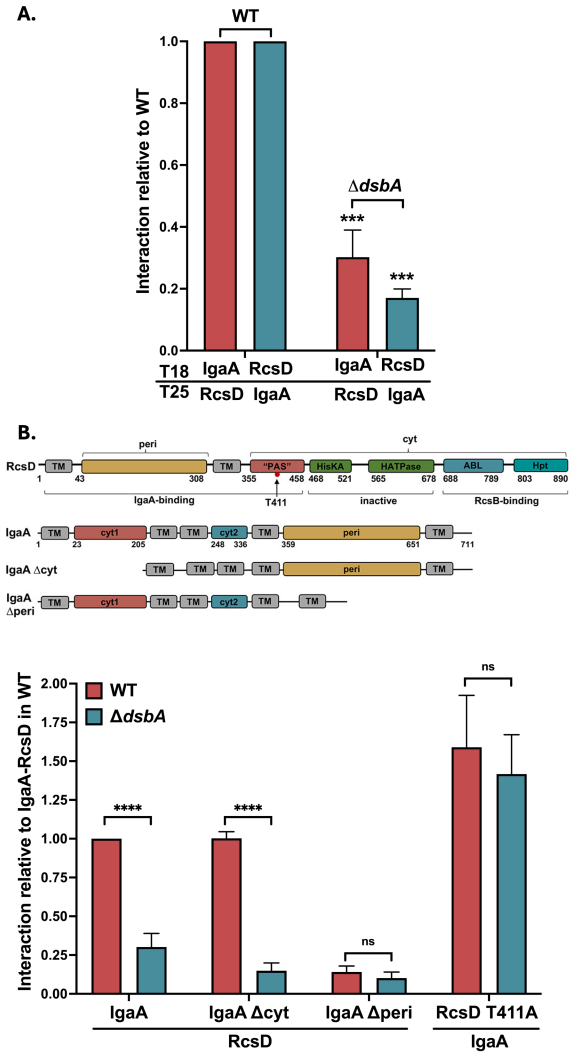

858

859

860

861

862

863

864

865

866 **Fig. 5:**

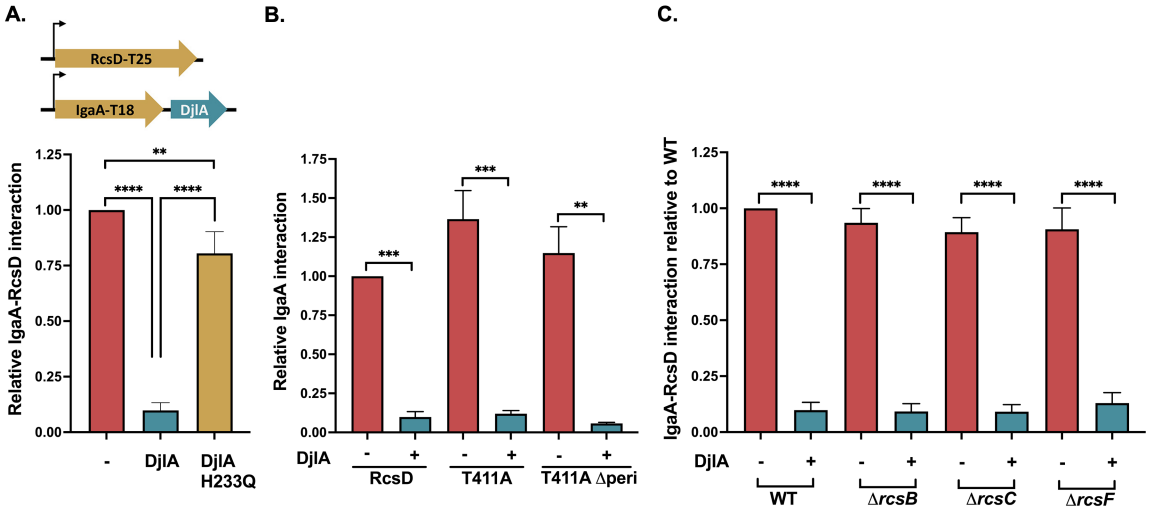

867

868

869

870

871

872

873

874

875

876

877

878

879

880

881

882

883

884 **Fig. 6:**

885

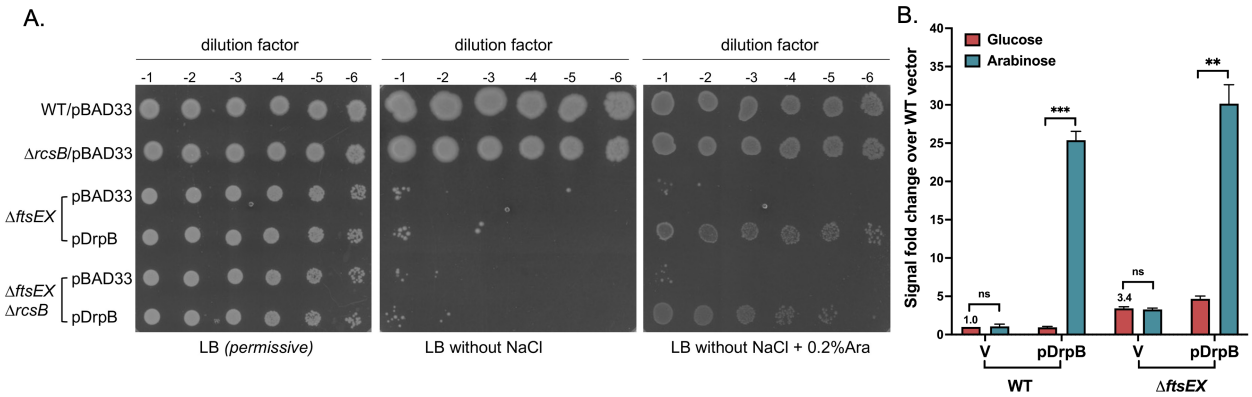

886

887

888

889

890

891

892

893

894

895

896

897

898

899

900

901

902 **Fig. 7:**

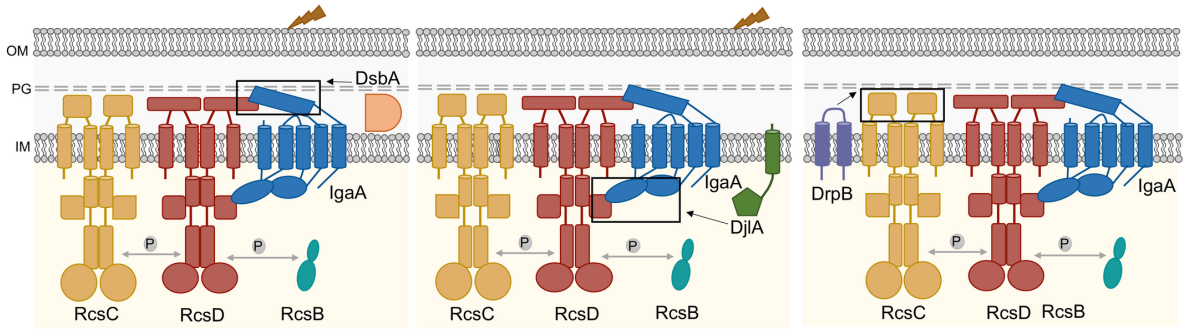

903

904

905

906 **References:**

907

908 1. Silhavy TJ, Kahne D, Walker S. The bacterial cell envelope. Cold Spring Harb Perspect
909 Biol. 2010;2(5):a000414. Epub 20100414. doi: 10.1101/cshperspect.a000414. PubMed
910 PMID: 20452953; PubMed Central PMCID: PMCPMC2857177.
911 2. Wall E, Majdalani N, Gottesman S. The Complex Rcs Regulatory Cascade. Annu Rev
912 Microbiol. 2018;72:111-39. Epub 20180613. doi: 10.1146/annurev-micro-090817-062640.
913 PubMed PMID: 29897834.
914 3. Gervais FG, Drapeau GR. Identification, cloning, and characterization of rcsF, a new
915 regulator gene for exopolysaccharide synthesis that suppresses the division mutation
916 ftsZ84 in Escherichia coli K-12. J Bacteriol. 1992;174(24):8016-22. doi:
917 10.1128/jb.174.24.8016-8022.1992. PubMed PMID: 1459951; PubMed Central PMCID:
918 PMCPMC207539.
919 4. Majdalani N, Gottesman S. The Rcs phosphorelay: a complex signal transduction
920 system. Annu Rev Microbiol. 2005;59:379-405. doi:
921 10.1146/annurev.micro.59.050405.101230. PubMed PMID: 16153174.
922 5. Castanié-Cornet MP, Cam K, Jacq A. RcsF is an outer membrane lipoprotein involved
923 in the RcsCDB phosphorelay signaling pathway in Escherichia coli. J Bacteriol.
924 2006;188(12):4264-70. doi: 10.1128/jb.00004-06. PubMed PMID: 16740933; PubMed
925 Central PMCID: PMCPMC1482940.
926 6. Laubacher ME, Ades SE. The Rcs phosphorelay is a cell envelope stress response
927 activated by peptidoglycan stress and contributes to intrinsic antibiotic resistance. J
928 Bacteriol. 2008;190(6):2065-74. Epub 20080111. doi: 10.1128/jb.01740-07. PubMed PMID:
929 18192383; PubMed Central PMCID: PMCPMC2258881.
930 7. Farris C, Sanowar S, Bader MW, Pfuetzner R, Miller SI. Antimicrobial peptides
931 activate the Rcs regulon through the outer membrane lipoprotein RcsF. J Bacteriol.
932 2010;192(19):4894-903. Epub 20100730. doi: 10.1128/jb.00505-10. PubMed PMID:
933 20675476; PubMed Central PMCID: PMCPMC2944553.
934 8. Cano DA, Domínguez-Bernal G, Tierrez A, Garcia-Del Portillo F, Casadesús J.
935 Regulation of capsule synthesis and cell motility in Salmonella enterica by the essential
936 gene igaA. Genetics. 2002;162(4):1513-23. doi: 10.1093/genetics/162.4.1513. PubMed
937 PMID: 12524328; PubMed Central PMCID: PMCPMC1462382.
938 9. Wall EA, Majdalani N, Gottesman S. IgaA negatively regulates the Rcs Phosphorelay
939 via contact with the RcsD Phosphotransfer Protein. PLoS Genet. 2020;16(7):e1008610.
940 Epub 20200727. doi: 10.1371/journal.pgen.1008610. PubMed PMID: 32716926; PubMed
941 Central PMCID: PMCPMC7418988.
942 10. Cho SH, Szewczyk J, Pesavento C, Zietek M, Banzhaf M, Roszczenko P, et al.
943 Detecting envelope stress by monitoring β-barrel assembly. Cell. 2014;159(7):1652-64. doi:
944 10.1016/j.cell.2014.11.045. PubMed PMID: 25525882.
945 11. Konovalova A, Mitchell AM, Silhavy TJ. A lipoprotein/β-barrel complex monitors
946 lipopolysaccharide integrity transducing information across the outer membrane. Elife.

947 2016;5. Epub 20160610. doi: 10.7554/eLife.15276. PubMed PMID: 27282389; PubMed
948 Central PMCID: PMCPMC4942254.
949 12. Zuber M, Hoover TA, Court DL. Analysis of a Coxiella burnetti gene product that
950 activates capsule synthesis in Escherichia coli: requirement for the heat shock chaperone
951 DnaK and the two-component regulator RcsC. J Bacteriol. 1995;177(15):4238-44. doi:
952 10.1128/jb.177.15.4238-4244.1995. PubMed PMID: 7635811; PubMed Central PMCID:
953 PMCPMC177168.
954 13. Kelley WL, Georgopoulos C. Positive control of the two-component RcsC/B signal
955 transduction network by DjlA: a member of the DnaJ family of molecular chaperones in
956 Escherichia coli. Mol Microbiol. 1997;25(5):913-31. doi: 10.1111/j.1365-
957 2958.1997.mmi527.x. PubMed PMID: 9364917.
958 14. Clavel T, Lazzaroni JC, Vianney A, Portalier R. Expression of the tolQRA genes of
959 Escherichia coli K-12 is controlled by the RcsC sensor protein involved in capsule synthesis.
960 Mol Microbiol. 1996;19(1):19-25. doi: 10.1046/j.1365-2958.1996.343880.x. PubMed PMID:
961 8821933.
962 15. Bury-Moné S, Nomane Y, Reymond N, Barbet R, Jacquet E, Imbeaud S, et al. Global
963 analysis of extracytoplasmic stress signaling in Escherichia coli. PLoS Genet.
964 2009;5(9):e1000651. Epub 20090918. doi: 10.1371/journal.pgen.1000651. PubMed PMID:
965 19763168; PubMed Central PMCID: PMCPMC2731931.
966 16. Potrykus J, Wegrzyn G. The ypdI gene codes for a putative lipoprotein involved in the
967 synthesis of colanic acid in Escherichia coli. FEMS Microbiol Lett. 2004;235(2):265-71. doi:
968 10.1016/j.femsle.2004.04.041. PubMed PMID: 15183873.
969 17. Tschowri N, Busse S, Hengge R. The BLUF-EAL protein YcgF acts as a direct anti-
970 repressor in a blue-light response of Escherichia coli. Genes Dev. 2009;23(4):522-34. doi:
971 10.1101/gad.499409. PubMed PMID: 19240136; PubMed Central PMCID:
972 PMCPMC2648647.
973 18. Westphal K, Langklotz S, Thomanek N, Narberhaus F. A trapping approach reveals
974 novel substrates and physiological functions of the essential protease FtsH in Escherichia
975 coli. J Biol Chem. 2012;287(51):42962-71. Epub 20121022. doi: 10.1074/jbc.M112.388470.
976 PubMed PMID: 23091052; PubMed Central PMCID: PMCPMC3522291.
977 19. Bittner LM, Westphal K, Narberhaus F. Conditional Proteolysis of the Membrane
978 Protein YfgM by the FtsH Protease Depends on a Novel N-terminal Degron. J Biol Chem.
979 2015;290(31):19367-78. Epub 20150619. doi: 10.1074/jbc.M115.648550. PubMed PMID:
980 26092727; PubMed Central PMCID: PMCPMC4521054.
981 20. Sikdar R, Simmons AR, Doerrler WT. Multiple envelope stress response pathways are
982 activated in an Escherichia coli strain with mutations in two members of the DedA
983 membrane protein family. J Bacteriol. 2013;195(1):12-24. Epub 20121005. doi:
984 10.1128/jb.00762-12. PubMed PMID: 23042993; PubMed Central PMCID:
985 PMCPMC3536178.
986 21. Majdalani N, Hernandez D, Gottesman S. Regulation and mode of action of the
987 second small RNA activator of RpoS translation, RprA. Mol Microbiol. 2002;46(3):813-26.
988 doi: 10.1046/j.1365-2958.2002.03203.x. PubMed PMID: 12410838.
989 22. Brill JA, Quinlan-Walshe C, Gottesman S. Fine-structure mapping and identification
990 of two regulators of capsule synthesis in Escherichia coli K-12. J Bacteriol.

991 1988;170(6):2599-611. doi: 10.1128/jb.170.6.2599-2611.1988. PubMed PMID: 2836365;
992 PubMed Central PMCID: PMCPMC211177.
993 23. Shiba Y, Miyagawa H, Nagahama H, Matsumoto K, Kondo D, Matsuoka S, et al.
994 Exploring the relationship between lipoprotein mislocalization and activation of the Rcs
995 signal transduction system in Escherichia coli. Microbiology (Reading). 2012;158(Pt
996 5):1238-48. Epub 20120209. doi: 10.1099/mic.0.056945-0. PubMed PMID: 22322964.
997 24. Heras B, Shouldice SR, Totsika M, Scanlon MJ, Schembri MA, Martin JL. DSB proteins
998 and bacterial pathogenicity. Nat Rev Microbiol. 2009;7(3):215-25. Epub 20090209. doi:
999 10.1038/nrmicro2087. PubMed PMID: 19198617.
1000 25. Bardwell JC, McGovern K, Beckwith J. Identification of a protein required for disulfide
1001 bond formation in vivo. Cell. 1991;67(3):581-9. doi: 10.1016/0092-8674(91)90532-4.
1002 PubMed PMID: 1934062.
1003 26. Kadokura H, Beckwith J. Four cysteines of the membrane protein DsbB act in concert
1004 to oxidize its substrate DsbA. Embo j. 2002;21(10):2354-63. doi:
1005 10.1093/emboj/21.10.2354. PubMed PMID: 12006488; PubMed Central PMCID:
1006 PMCPMC126001.
1007 27. Berkmen M, Boyd D, Beckwith J. The nonconsecutive disulfide bond of Escherichia
1008 coli phytase (AppA) renders it dependent on the protein-disulfide isomerase, DsbC. J Biol
1009 Chem. 2005;280(12):11387-94. Epub 20050110. doi: 10.1074/jbc.M411774200. PubMed
1010 PMID: 15642731.
1011 28. Missiakas D, Georgopoulos C, Raina S. Identification and characterization of the
1012 Escherichia coli gene dsbB, whose product is involved in the formation of disulfide bonds in
1013 vivo. Proc Natl Acad Sci U S A. 1993;90(15):7084-8. doi: 10.1073/pnas.90.15.7084. PubMed
1014 PMID: 7688471; PubMed Central PMCID: PMCPMC47080.
1015 29. Dailey FE, Berg HC. Mutants in disulfide bond formation that disrupt flagellar
1016 assembly in Escherichia coli. Proc Natl Acad Sci U S A. 1993;90(3):1043-7. doi:
1017 10.1073/pnas.90.3.1043. PubMed PMID: 8503954; PubMed Central PMCID:
1018 PMCPMC45807.
1019 30. Kadokura H, Tian H, Zander T, Bardwell JC, Beckwith J. Snapshots of DsbA in action:
1020 detection of proteins in the process of oxidative folding. Science. 2004;303(5657):534-7.
1021 doi: 10.1126/science.1091724. PubMed PMID: 14739460.
1022 31. Leverrier P, Declercq JP, Denoncin K, Vertommen D, Hiniker A, Cho SH, Collet JF.
1023 Crystal structure of the outer membrane protein RcsF, a new substrate for the periplasmic
1024 protein-disulfide isomerase DsbC. J Biol Chem. 2011;286(19):16734-42. Epub 20110316.
1025 doi: 10.1074/jbc.M111.224865. PubMed PMID: 21454485; PubMed Central PMCID:
1026 PMCPMC3089515.
1027 32. Rogov VV, Rogova NY, Bernhard F, Löhr F, Dötsch V. A disulfide bridge network within
1028 the soluble periplasmic domain determines structure and function of the outer membrane
1029 protein RCSF. J Biol Chem. 2011;286(21):18775-83. Epub 20110406. doi:
1030 10.1074/jbc.M111.230185. PubMed PMID: 21471196; PubMed Central PMCID:
1031 PMCPMC3099694.
1032 33. Pucciarelli MG, Rodríguez L, García-Del Portillo F. A Disulfide Bond in the Membrane
1033 Protein IgaA Is Essential for Repression of the RcsCDB System. Front Microbiol.

1034 2017;8:2605. Epub 20171222. doi: 10.3389/fmicb.2017.02605. PubMed PMID: 29312270;
1035 PubMed Central PMCID: PMCPMC5744062.
1036 34. Battesti A, Bouveret E. The bacterial two-hybrid system based on adenylate cyclase
1037 reconstitution in Escherichia coli. Methods. 2012;58(4):325-34. Epub 20120724. doi:
1038 10.1016/j.ymeth.2012.07.018. PubMed PMID: 22841567.
1039 35. Karimova G, Pidoux J, Ullmann A, Ladant D. A bacterial two-hybrid system based on
1040 a reconstituted signal transduction pathway. Proc Natl Acad Sci U S A. 1998;95(10):5752-6.
1041 doi: 10.1073/pnas.95.10.5752. PubMed PMID: 9576956; PubMed Central PMCID:
1042 PMCPMC20451.
1043 36. Watanabe N, Savchenko A. Molecular insights into the initiation step of the Rcs
1044 signaling pathway. Structure. 2024. Epub 20240625. doi: 10.1016/j.str.2024.06.003.
1045 PubMed PMID: 38964336.
1046 37. Clarke DJ, Jacq A, Holland IB. A novel DnaJ-like protein in Escherichia coli inserts into
1047 the cytoplasmic membrane with a type III topology. Mol Microbiol. 1996;20(6):1273-86. doi:
1048 10.1111/j.1365-2958.1996.tb02646.x. PubMed PMID: 8809778.
1049 38. Alekhina O, Valkovicova L, Turna J. Study of membrane attachment and in vivo co-
1050 localization of TerB protein from uropathogenic Escherichia coli KL53. Gen Physiol Biophys.
1051 2011;30(3):286-92. doi: 10.4149/gpb_2011_03_286. PubMed PMID: 21952438.
1052 39. Anantharaman V, Iyer LM, Aravind L. Ter-dependent stress response systems: novel
1053 pathways related to metal sensing, production of a nucleoside-like metabolite, and DNA-
1054 processing. Mol Biosyst. 2012;8(12):3142-65. doi: 10.1039/c2mb25239b. PubMed PMID:
1055 23044854; PubMed Central PMCID: PMCPMC4104200.
1056 40. Genevaux P, Wawrzynow A, Zylicz M, Georgopoulos C, Kelley WL. DjlA is a third DnaK
1057 co-chaperone of Escherichia coli, and DjlA-mediated induction of colanic acid capsule
1058 requires DjlA-DnaK interaction. J Biol Chem. 2001;276(11):7906-12. Epub 20001205. doi:
1059 10.1074/jbc.M003855200. PubMed PMID: 11106641.
1060 41. Bernard S, Clarke DJ, Chen MX, Holland IB, Jacq A. Increased sensitivity of E. coli to
1061 novobiocin, EDTA and the anticalmodulin drug W7 following overproduction of DjlA requires
1062 a functional transmembrane domain. Mol Gen Genet. 1998;259(6):645-55. doi:
1063 10.1007/pl00008629. PubMed PMID: 9819058.
1064 42. Clarke DJ, Holland IB, Jacq A. Point mutations in the transmembrane domain of DjlA,
1065 a membrane-linked DnaJ-like protein, abolish its function in promoting colanic acid
1066 production via the Rcs signal transduction pathway. Mol Microbiol. 1997;25(5):933-44. doi:
1067 10.1111/j.1365-2958.1997.mmi528.x. PubMed PMID: 9364918.
1068 43. Genevaux P, Schwager F, Georgopoulos C, Kelley WL. The djlA gene acts
1069 synergistically with dnaJ in promoting Escherichia coli growth. J Bacteriol.
1070 2001;183(19):5747-50. doi: 10.1128/jb.183.19.5747-5750.2001. PubMed PMID: 11544239;
1071 PubMed Central PMCID: PMCPMC95468.
1072 44. Toutain CM, Clarke DJ, Leeds JA, Kuhn J, Beckwith J, Holland IB, Jacq A. The
1073 transmembrane domain of the DnaJ-like protein DjlA is a dimerisation domain. Mol Genet
1074 Genomics. 2003;268(6):761-70. Epub 20030131. doi: 10.1007/s00438-002-0793-z. PubMed
1075 PMID: 12655402.
1076 45. Yahashiri A, Babor JT, Anwar AL, Bezy RP, Piette EW, Arends SJR, et al. DrpB (YedR) Is
1077 a Nonessential Cell Division Protein in Escherichia coli. J Bacteriol. 2020;202(23). Epub

1078 20201104. doi: 10.1128/jb.00284-20. PubMed PMID: 32900831; PubMed Central PMCID:
1079 PMCPMC7648144.
1080 46. Schmidt KL, Peterson ND, Kustusch RJ, Wissel MC, Graham B, Phillips GJ, Weiss DS.
1081 A predicted ABC transporter, FtsEX, is needed for cell division in Escherichia coli. J Bacteriol.
1082 2004;186(3):785-93. doi: 10.1128/jb.186.3.785-793.2004. PubMed PMID: 14729705;
1083 PubMed Central PMCID: PMCPMC321481.
1084 47. Yang DC, Peters NT, Parzych KR, Uehara T, Markovski M, Bernhardt TG. An ATP-
1085 binding cassette transporter-like complex governs cell-wall hydrolysis at the bacterial
1086 cytokinetic ring. Proc Natl Acad Sci U S A. 2011;108(45):E1052-60. Epub 20111017. doi:
1087 10.1073/pnas.1107780108. PubMed PMID: 22006326; PubMed Central PMCID:
1088 PMCPMC3215046.
1089 48. Du S, Pichoff S, Lutkenhaus J. FtsEX acts on FtsA to regulate divisome assembly and
1090 activity. Proc Natl Acad Sci U S A. 2016;113(34):E5052-61. Epub 20160808. doi:
1091 10.1073/pnas.1606656113. PubMed PMID: 27503875; PubMed Central PMCID:
1092 PMCPMC5003251.
1093 49. Lee J, Page R, García-Contreras R, Palermino JM, Zhang XS, Doshi O, et al. Structure
1094 and function of the Escherichia coli protein YmgB: a protein critical for biofilm formation and
1095 acid-resistance. J Mol Biol. 2007;373(1):11-26. Epub 20070802. doi:
1096 10.1016/j.jmb.2007.07.037. PubMed PMID: 17765265; PubMed Central PMCID:
1097 PMCPMC2185545.
1098 50. Kettles RA, Tschowri N, Lyons KJ, Sharma P, Hengge R, Webber MA, Grainger DC. The
1099 Escherichia coli MarA protein regulates the ycgZ-ymgABC operon to inhibit biofilm
1100 formation. Mol Microbiol. 2019;112(5):1609-25. Epub 20190929. doi: 10.1111/mmi.14386.
1101 PubMed PMID: 31518447; PubMed Central PMCID: PMCPMC6900184.
1102 51. Palmer AD, Slauch JM. Envelope Stress and Regulation of the Salmonella
1103 Pathogenicity Island 1 Type III Secretion System. J Bacteriol. 2020;202(17). Epub 20200810.
1104 doi: 10.1128/jb.00272-20. PubMed PMID: 32571967; PubMed Central PMCID:
1105 PMCPMC7417839.
1106 52. Shiba Y, Matsumoto K, Hara H. DjlA negatively regulates the Rcs signal transduction
1107 system in Escherichia coli. Genes Genet Syst. 2006;81(1):51-6. doi: 10.1266/ggs.81.51.
1108 PubMed PMID: 16607041.
1109 53. Jacob-Dubuisson F, Mechaly A, Betton JM, Antoine R. Structural insights into the
1110 signalling mechanisms of two-component systems. Nat Rev Microbiol. 2018;16(10):585-93.
1111 doi: 10.1038/s41579-018-0055-7. PubMed PMID: 30008469.
1112 54. Mascher T, Helmann JD, Unden G. Stimulus perception in bacterial signal-
1113 transducing histidine kinases. Microbiol Mol Biol Rev. 2006;70(4):910-38. doi:
1114 10.1128/mmbr.00020-06. PubMed PMID: 17158704; PubMed Central PMCID:
1115 PMCPMC1698512.
1116 55. Krell T, Lacal J, Busch A, Silva-Jiménez H, Guazzaroni ME, Ramos JL. Bacterial sensor
1117 kinases: diversity in the recognition of environmental signals. Annu Rev Microbiol.
1118 2010;64:539-59. doi: 10.1146/annurev.micro.112408.134054. PubMed PMID: 20825354.
1119 56. Schumacher K, Gelhausen R, Kion-Crosby W, Barquist L, Backofen R, Jung K.
1120 Ribosome profiling reveals the fine-tuned response of Escherichia coli to mild and severe
1121 acid stress. mSystems. 2023;8(6):e0103723. Epub 20231101. doi:

1122 10.1128/msystems.01037-23. PubMed PMID: 37909716; PubMed Central PMCID:
1123 PMCPMC10746267.
1124 57. Flores-Kim J, Darwin AJ. The Phage Shock Protein Response. Annu Rev Microbiol.
1125 2016;70:83-101. Epub 20160608. doi: 10.1146/annurev-micro-102215-095359. PubMed
1126 PMID: 27297125.
1127 58. Todor H, Herrera N, Gross CA. Three Bacterial DedA Subfamilies with Distinct
1128 Functions and Phylogenetic Distribution. mBio. 2023;14(2):e0002823. Epub 20230301. doi:
1129 10.1128/mbio.00028-23. PubMed PMID: 36856409; PubMed Central PMCID:
1130 PMCPMC10127716.
1131 59. Baba T, Ara T, Hasegawa M, Takai Y, Okumura Y, Baba M, et al. Construction of
1132 Escherichia coli K-12 in-frame, single-gene knockout mutants: the Keio collection. Mol Syst
1133 Biol. 2006;2:2006.0008. Epub 20060221. doi: 10.1038/msb4100050. PubMed PMID:
1134 16738554; PubMed Central PMCID: PMCPMC1681482.
1135 60. Gibson DG, Young L, Chuang RY, Venter JC, Hutchison CA, 3rd, Smith HO. Enzymatic
1136 assembly of DNA molecules up to several hundred kilobases. Nat Methods. 2009;6(5):343-
1137 5. Epub 20090412. doi: 10.1038/nmeth.1318. PubMed PMID: 19363495.
1138 61. Ulbrandt ND, Newitt JA, Bernstein HD. The E. coli signal recognition particle is
1139 required for the insertion of a subset of inner membrane proteins. Cell. 1997;88(2):187-96.
1140 doi: 10.1016/s0092-8674(00)81839-5. PubMed PMID: 9008159.
1141

1142

1143 **Supplementary Figure legends:**

1144 **Fig. S1: Signaling by putative RcsF-independent Rcs activators.** A genomic library was transformed
1145 into an *rcsF* deletion strain (EAW34) containing the P_{rprA}::mCherry reporter for Rcs signaling and the
1146 colonies were screened for increased fluorescence. The plasmids were isolated from colonies showing high
1147 fluorescence (indicating Rcs activation) and sequenced. The genes present in the candidate plasmids,
1148 representing two genomic regions, are shown here. **A.** The gene encoding the YedR/DrpB ORF (indicated
1149 here in red) was present in 13 out of 14 candidate plasmids, in 8 independent clones with different end
1150 points. **B.** The remaining candidate plasmid contained genes for spot42 sRNA (*spf*) and the YihA ORF. **C.**
1151 For this P_{rprA}::mCherry assay, the strain AP 51 (*rcsF::kan*) overexpressing pBR-plac (V), pBR-plac-*rseX*
1152 or pBR-plac-*spf* was grown in MOPS minimal glycerol medium containing 100 μg/ml ampicillin and their
1153 fluorescence measured over time at 37°C. The RFU at OD 0.4 is plotted with the value for the vector in the
1154 absence of IPTG set to 1. The strains were induced with 100 μM IPTG. **D.** The AP51 strain containing
1155 pBAD33 or pBAD33-*yihA* (pAP3327) was grown in MOPS minimal glycerol medium with 25 μg/ml
1156 chloramphenicol and induced with 0.02% arabinose. Data from three independent experiments is plotted as
1157 mean with error bars indicating the standard deviation. Values were statistically analyzed using multiple
1158 unpaired *t*-tests. 'ns' indicates a *P*-value > 0.05 (non- significant).

1159

1160 **Fig. S2: Dependence of DsbA, DjlA, and DrpB on each other for Rcs activation: A. Effect of DjlA or**
1161 **DrpB deletion upon Rcs signaling in *dsbA* mutants:** All the strains carry an *rprA* promoter fusion to
1162 mCherry (P_{rprA}-mCherry) and the mCherry fluorescence acts as an indicator for Rcs activation. For the
1163 P_{rprA}::mCherry assay, the cells were grown in MOPS minimal glucose medium at 37°C. The RFU at OD
1164 0.4 for the WT uninduced was set to 1 and the relative induction compared to that depicted here (top panel).
1165 The cells were treated at the beginning of growth with either 1mM DTT or 20μg/ml PMBN. Strains used
1166 were: WT (EAW8), Δ*dsbA djlA::kan* (AP72), and Δ*dsbA drpB::kan* (AP71). The middle panel depicts the
1167 relative fluorescence units (RFU) as a function of time and the lower panel shows a representative growth

1168 curve for each strain. **B. Signaling upon overexpression of DjlA or DrpB in *dsbA* mutants:** The strains
1169 WT (EAW8) and *dsbA::kan* (EAW62) carry the P_{rprA}::mCherry promoter fusion. The strains containing
1170 plasmids overexpressing DjlA (pDjlA/pPSG961) or DrpB (pDrpB/pDSW1977) were grown in MOPS
1171 minimal glycerol medium with 25 μg/ml chloramphenicol at 37°C and 0.02% arabinose was added for
1172 induction. The RFU at OD 0.4 for the WT vector uninduced was set to one; other results are normalized to
1173 that value. The middle and bottom panels depict the RFU and OD_{600} as a function of time. **C. Rcs activation**
1174 **by overexpression of DjlA and DrpB in Δ*drpB* and Δ*djlA* strains:** The strains overexpressing DjlA
1175 (pDjlA/pPSG961) or DrpB (pDrpB/pDSW1977) were grown as in B. Strains used were: WT (EAW8),
1176 *drpB::kan* (AP41), and *djlA::kan* (AP46). Data from three independent experiments is plotted as mean with
1177 error bars indicating the standard deviation. Values were statistically analyzed using multiple unpaired *t*-
1178 tests. Statistical significance is indicated as follows: ns ($P > 0.05$; non- significant), * ($P < 0.05$), ** ($P \leq$
1179 0.01), *** ($P \leq 0.001$).
1180
1181 **Fig. S3: Signaling by multicopy RcsF.** The strains overexpressing RcsF (pAP3340) or its inner membrane
1182 localized mutant $RcsF^{IM}$ (pAP3341) were grown in MOPS minimal glycerol medium containing
1183 chloramphenicol (25 μg/ml) and either 0.2% glucose or 0.02% arabinose at 37°C. The RFU at OD 0.4
1184 compared to the uninduced vector control, set to 1, was plotted. The strains used were: WT (EAW8),
1185 *rcsF::kan* (AP51), *rcsC* Δ*peri* (EAW70), and *rcsD T411A* (EAW121).
1186
1187 **Fig. S4: A. Δ*dsbA* does not respond to A22 and Mecillinam.** For the P_{rprA}::mCherry assay, the strains
1188 were grown in MOPS minimal glucose medium at 37°C. The RFU at OD 0.4 as compared to WT uninduced,
1189 set to 1, is depicted here. The cells were subjected to either 5 μg/ml A22 or 0.3 μg/ml mecillinam. The
1190 strains used were: WT (EAW8), *rcsF::cat* (EAW32), *dsbA::kan* (EAW62), and *dsbA::kan rcsF::cat*
1191 (EAW67). **B. Rcs signaling in RcsC cysteine mutant strains.** For the P_{rprA}::mCherry assay, the strains
1192 were grown in MOPS minimal glucose medium at 37°C. The RFU at OD 0.4 as compared to WT uninduced,

1193 set to one, is shown here. The cells were subjected to either 1mM DTT or 20µg/ml PMBN. The *dsbA* RcsC
1194 C2A (*rcsC* C111A C154A) mutant responded to DTT and PMBN similarly to the Δ*dsbA* strain. The strains
1195 used were: WT (EAW8), *dsbA::kan* (EAW62), *rcsC C2A atoS::kan* (AP172), and Δ*dsbA rcsC C2A*
1196 *atoS::kan* (AP173). **C. Interaction of IgaA Cysteine mutants with RcsD.** Beta-galactosidase activity was
1197 measured in bacterial two hybrid assay, in the standard Δ*cyaA* strain (BTH101 or in a strain deleted for both
1198 *cyaA* and *dsbA*, AP 58 (BTH101 Δ*dsbA*)). The IgaA-RcsD interaction in WT was normalized to 1 and other
1199 interactions plotted relative to this interaction. This data is compiled from separate sets of assays, each
1200 normalized relative to the IgaA/RcsD signal in that experiment. The T18 tagged plasmids used are pEAW1
1201 (IgaA-T18), pAP102 (IgaA C404S C425S), pAP103 (IgaA C498S C504S), pEAW1C4S (IgaA C4S)
1202 pEAW1peri (IgaA Δperi), pEAW8 (RcsD-T25), and pEAW8T (RcsD T411A-T25). See Fig. 4B for IgaA
1203 Δperi structure. **D. Expression of IgaA-T18 fusions.** EAW8 (WT) and EAW62 (Δ*dsbA*) expressing the
1204 IgaA-T18 fusion constructs were probed with the anti-CyaA antibody and anti-EF-Tu antibody (loading
1205 control). Lane 1 shows the protein markers; Lanes 2-5 and Lanes 6-9 show expression in EAW8 and
1206 EAW62 respectively. Lanes 2, 6: pEAW1 (IgaA), Lanes 3, 7: pAP101 (IgaA Δcyt), Lanes 4, 8: pEAW1peri
1207 (IgaA Δperi), and Lanes 5, 9: pEAW1C4S (IgaA C4S). See Fig. 4B for structures of IgaA Δcyt and IgaA
1208 Δperi. **E. Signaling by IgaA cysteine mutants.** For the P_{rprA}::mCherry assay, the strains EAW19 (Δ*rcsD*),
1209 AP168 (*igaA C4S* Δ*rcsD*), and AP169 (Δ*rcsD dsbA::kan)* were transformed with RcsD (pEAW11) and
1210 plated on LB Ampicillin plates. The resulting transformed colonies were inoculated without further
1211 purification in LB medium (with Ampicillin) and their fluorescence monitored at 37°C. The cells were
1212 subjected to nothing (uninduced) or to 1mM DTT from the beginning. The RFU/OD after 6h of growth is
1213 plotted and the OD at that time point is shown for each bar. The growth profile of the strains during the
1214 experiment is shown on the right. Statistical significance was calculated using multiple unpaired *t*-tests and
1215 is indicated as follows: ns ($P > 0.05$; non- significant), * ($P < 0.05$), ** ($P \leq 0.01$), *** ($P \leq 0.001$), and
1216 **** ($P \leq 0.0001$).
1217

1218 **Fig. S5: DjlA TM helix does not recognize a Rcs target. A. DjlA signaling in a RcsC$_{MalF}$ strain:** For
1219 the P$_{rprA}$::mCherry assay, the strains WT (EAW8) and RcsC$_{MalF}$ (EAW72) overexpressing DjlA
1220 (pDjlA/pPSG961) or pBAD33 vector were grown in MOPS minimal glycerol medium containing
1221 chloramphenicol (25 μg/ml) and either 0.2% glucose or 0.02% arabinose at 37°C. The RFU at OD 0.4
1222 uninduced for the WT was set to 1 (first column), and relative values to that are plotted. EAW72 carries a
1223 chimeric variant of RcsC which has its cytoplasmic domains fused to the MalF TM helices. Statistical
1224 significance was calculated using multiple unpaired *t*-tests and is indicated as follows: ns ($P > 0.05$; non-
1225 significant), * ($P < 0.05$), ** ($P \leq 0.01$), *** ($P \leq 0.001$), and **** ($P \leq 0.0001$). **B. Signaling by DjlA**
1226 **mutants:** For the P$_{rprA}$::mCherry assay, the strain AP 163 (*djlA::kan* Δ*rcsF*) carrying the pBAD33 vector
1227 or pBAD33 derivatives expressing DjlA (pDjlA/pPSG961), DjlA H233Q (pAP3315), DjlA ΔTM
1228 (pAP3311), or DjlA$_{MalF}$ (pAP3312) were grown as in A. The RFU of the strain carrying the uninduced
1229 vector at OD 0.4 was set to 1 and results normalized to that are plotted. **C. The DjlA TM helix is not**
1230 **needed for weakening IgaA-RcsD interactions.** Beta-galactosidase activity was measured in a Δ*cyaA*
1231 strain (BTH101). IgaA and RcsD/RcsD T411A were fused to the T18 and T25 domains, respectively. DjlA
1232 or its variants were cloned downstream of IgaA under the same promoter control. IgaA-RcsD interaction
1233 in the absence of DjlA was normalized to 1 and all other interactions are plotted relative to this interaction**.**
1234 Plasmids used were pEAW1 (IgaA-T18), pEAW8 (RcsD-T25), pAP101 (IgaA Δcyt –T18), pAP1401
1235 (IgaA-T18 + DjlA), pAP1403 (IgaA-T18 + DjlA ΔTM), and pAP1404 (IgaA-T18 + DjlA$_{MalF}$). **D.**
1236 **Expression of IgaA-T18 fusion.** *E. coli* DH5α strain expressing the IgaA-T18 fusion constructs were
1237 probed with the anti-CyaA antibody and anti-EF-Tu antibody (loading control). Lane 1: protein marker;
1238 Lane 2: pEAW1 (IgaA-T18), Lane 3: pAP1401 (IgaA-T18 + DjlA), Lane 4: pAP1403 (IgaA-T18 + DjlA
1239 ΔTM).
1240
1241 **Fig. S6: Rcs signaling in Δ*djlA*. A. Dose-dependent PMBN response in Δ*djlA*:** For the P$_{rprA}$::mCherry
1242 assay, the strains WT (EAW8) and *djlA::kan* (AP46) were grown in MOPS minimal glucose medium with

1243 or without PMBN (5 μg/ml, 10 μg/ml, or 20 μg/ml) at 37°C. The RFU at OD 0.4 as compared to WT
1244 uninduced, set to 1, is depicted here. Values (Mean ± SD) from independent experiments were statistically
1245 analyzed using multiple unpaired *t*-tests. The fluorescence signal of each PMBN dose in Δ*djlA* was
1246 compared to the RFU signal of the WT strain at the same dose. Statistical significance for this comparison
1247 is indicated as follows: ns ($P > 0.05$; non- significant), * ($P \leq 0.05$). **B. Δ*djlA* responds to A22 and**
1248 **Mecillinam:** For the P_{rprA}::mCherry assay, the strains WT (EAW8) and *djlA::kan* (AP46) were grown in
1249 MOPS minimal glucose medium and treated with nothing (uninduced) or with PMBN (20 μg/ml), MreB
1250 inhibitor A22 (5 μg/ml), or Mecillinam (0.3 μg/ml, Mec) at 37°C. The RFU at OD 0.4 as compared to WT
1251 uninduced, set to 1, is plotted. For statistical analysis, the RFU with each chemical treatment in Δ*djlA* was
1252 compared to the RFU signal of the WT strain for that compound. **C. PMBN response in Δ*djlA* at 42°C:**
1253 For the P_{rprA}::mCherry assay, the strains WT (EAW8) and *djlA::kan* (AP46) were grown in MOPS minimal
1254 glucose medium with or without PMBN (20 μg/ml) at 42°C. The RFU at OD 0.4 as compared to WT
1255 uninduced is plotted. The statistical analysis shows the comparison between signals of Δ*djlA* and WT. **D.**
1256 **IgaA-RcsD interactions in Δ*djlA* :** The IgaA-RcsD interaction was tested using BACTH in BTH101 (WT)
1257 and AP 63 (*BTH 101* Δ*djlA*). Plasmids used were pEAW1 (IgaA-T18), pEAW8 (RcsD-T25), pEAW2
1258 (IgaA-T25), pEAW7 (RcsD-T18), pEAW8peri (RcsD Δperi-T25), and pEAW8T (T411A). IgaA-RcsD
1259 interaction in WT was normalized to 1 and the interaction in Δ*djlA* (AP63) is plotted relative to this
1260 interaction**.** Statistical analysis using multiple unpaired *t*-tests is indicated as follows: ns ($P > 0.05$; non-
1261 significant), * ($P \leq 0.05$).
1262
1263 **Fig. S7: Characterization of DrpB mutants. A. Signaling by DrpB mutants in Δ*rcsF*:** For the
1264 P_{rprA}::mCherry assay, the *rcsF::kan* (AP51) strain was transformed with the pBAD33 vector or pBAD33
1265 plasmids carrying DrpB (pDSW1977), DrpB $\Delta peri_{48\text{-}57}$ (pAP3301), DrpB C29A (pAP3304), DrpB R38F
1266 (pAP3305), DrpB G83A (pAP3306), or DrpB T89A (pAP3307). The transformed strains were grown in
1267 MOPS minimal glycerol medium containing chloramphenicol (25 μg/ml) and either 0.2% glucose or 0.02%

1268 arabinose at 37°C. The RFU at OD 0.4 is plotted relative to the uninduced WT, set to 1. **B. Analysis of**
1269 **DrpB mutants as *ftsEX* suppressors:** The strains WT (EC251) and Δ*ftsEX* (EC1215) were transformed
1270 with the same plasmids as in A and grown overnight in LB Miller media with chloramphenicol at 37°C.
1271 The cultures were then normalized to OD_{600} 1 and 4 ul was spotted on LB Miller (permissive), LBON (LB
1272 without NaCl) or LBON (with 0.2% arabinose). Plates were imaged after 16h incubation at 37°C.
1273
1274 **Fig. S8: Analysis of DrpB-dependent signaling**. **A. DrpB interactions with Rcs components:** The
1275 interaction of DrpB with IgaA, RcsD, and RcsC was tested using the BACTH assay in BTH101. The IgaA-
1276 RcsD interaction was normalized to 1 and the other interactions were plotted relative to this interaction**.** No
1277 significant interaction of RcsC was observed with RcsD or DrpB. Plasmids used were pEAW2 (IgaA-T25),
1278 pEAW8 (RcsD-T25), pEAW6 (RcsC-T25), pEAW7 (RcsD-T18), pAP407 (DrpB-T18), pAP408 (DrpB-
1279 T25), and pKNT25 vector. Values (Mean ± SD) from independent experiments were statistically analyzed
1280 using multiple unpaired *t*-tests. 'ns' indicates a *P*-value > 0.05 (non- significant). **B. Rcs signaling by**
1281 **Δ*drpB*:** For the P_{rprA}::mCherry assay, **t**he strains WT (EAW8) and *drpB::kan* (AP41) were grown in MOPS
1282 minimal glucose medium and treated with nothing (uninduced) or with PMBN (20 µg/ml), MreB inhibitor
1283 A22 (5 µg/ml), or Mecillinam (0.3 µg/ml, Mec) at 18°C. The RFU at OD 0.4 as compared to WT uninduced,
1284 set to 1, is plotted. The statistical analysis compared the signals of Δ*drpB* and WT for each condition. **C.**
1285 **DrpB signaling is independent of the *psp* pathway.** For this P_{rprA}::mCherry assay, the WT (EAW8),
1286 *pspC::kan* (AP113) and *pspF::kan* (AP114) strains transformed with pBAD33 vector or pDrpB
1287 (pDSW1977) were grown in MOPS minimal glycerol medium containing chloramphenicol (25 µg/ml)
1288 either 0.2% glucose or 0.02% arabinose at 37°C. The RFU at OD 0.4 is plotted relative to uninduced WT,
1289 set to 1. Statistical analysis was done using multiple unpaired *t*-tests and *P*-value for comparison with the
1290 uninduced vector control of each strain is indicated as follows: ns ($P > 0.05$; non- significant) and *** (P
1291 ≤ 0.001).
1292

1293 **Fig. S9: Signaling by multicopy YmgB.** For the P_{rprA}::mCherry assay, strains overexpressing the pBAD33
1294 vector (V) or pBAD33-YmgB (pAP3325) were grown in MOPS minimal glycerol medium containing
1295 chloramphenicol (25 μg/ml) and either 0.2% glucose or 0.02% arabinose at 37°C. The RFU at OD 0.4
1296 relative to the uninduced vector control, set to 1, is plotted here. The strains used are: WT (EAW8),
1297 *rcsF::kan* (AP51), *rcsC* Δ*peri* (EAW70), and *rcsD T411A* (EAW121).
1298